Matter

CellPress

Article

High-strength and ultra-tough whole spider silk fibers spun from transgenic silkworms

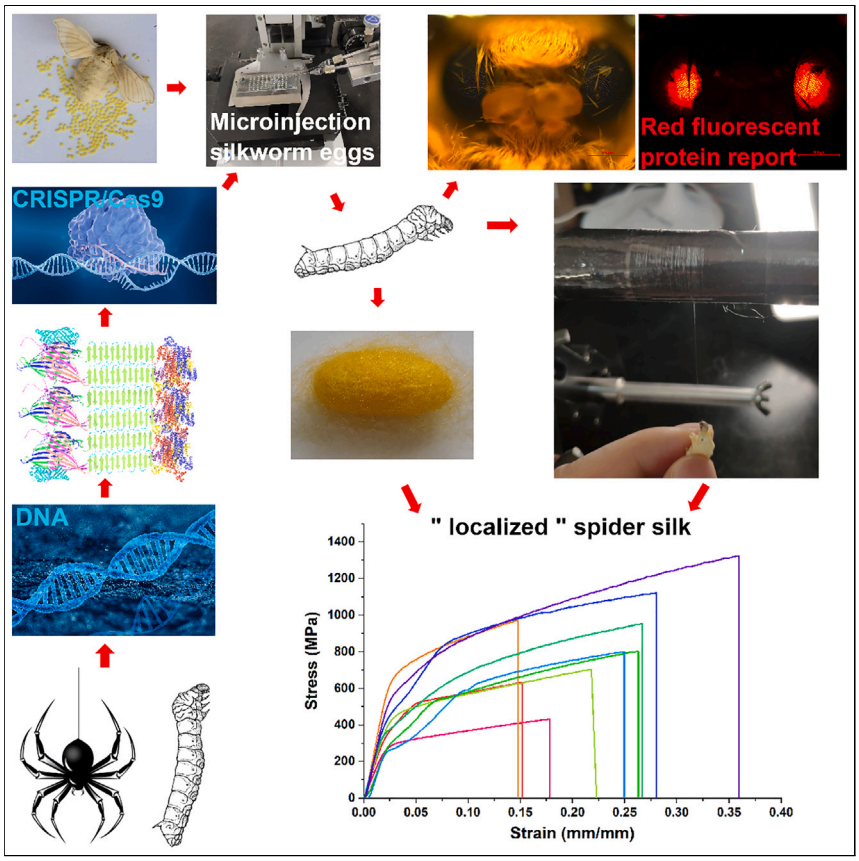

Developing sustainable materials with high strength and ultra-toughness is vital for ecological civilization. Using transgenic silkworms, we have successfully produced the first full-length spider silk, overcoming the scientific challenge of understanding the essence of toughness and strength. The resulting bionic spider silk exhibits high strength (1,299 MPa) and ultra-toughness (319 MJ/m^3), offering a potentially sustainable substitute for synthetic commercial fibers. This breakthrough provides valuable insights for the development of super materials, including those for a space elevator, driving the advancement of civilization.

Junpeng Mi, Yizhong Zhou, Sanyuan Ma, ..., Suyang Wang, Luyang Tian, Qing Meng

xiaqy@swu.edu.cn (Q.X.)
mengqing@dhu.edu.cn (Q.M.)

Highlights

Unraveled the fundamental factors governing material toughness and strength

The minimum basic structure model of silkworm silk (Fib-H_{12}Fib-$L_{12}P25_2$) is proposed

The first whole full-length spider silk fiber obtained by transgenic silkworms

Bionic spider silk combines high strength (1,299 MPa) and super toughness (319 MJ/m^3)

2 **Benchmark**
First qualification/assessment of material properties and/or performance

Mi et al., Matter 6, 1–23
October 4, 2023
https://doi.org/10.1016/j.matt.2023.08.013

Please cite this article in press as: Mi et al., High-strength and ultra-tough whole spider silk fibers spun from transgenic silkworms, Matter (2023), https://doi.org/10.1016/j.matt.2023.08.013

Matter

CellPress

Article

High-strength and ultra-tough whole spider silk fibers spun from transgenic silkworms

Junpeng Mi,[1,5] Yizhong Zhou,[1] Sanyuan Ma,[2] Xingping Zhou,[1] Shouying Xu,[1] Yuchen Yang,[3] Yuan Sun,[1] Qingyou Xia,[4,*] Hongnian Zhu,[1] Suyang Wang,[1] Luyang Tian,[1] and Qing Meng[1,*]

SUMMARY

To advance ecological civilization, developing sustainable, eco-friendly high-strength and ultra-tough alternatives to non-sustainable synthetic fibers, such as nylon, is crucial. This necessitates a deeply scientific understanding of the fundamental determinants of fiber strength and toughness, as well as overcoming engineering challenges for cost-effective, large-scale production of high-performance silk fibers. Inspired by the mechanical properties of polyamide fibers, including nylon and Kevlar, we employed CRISPR-Cas9-mediated gene editing to successfully synthesize whole polyamide spider silk fibers from transgenic silkworms. These fibers exhibited impressive tensile strength (1,299 MPa) and toughness (319 MJ/m^3), surpassing Kevlar's toughness 6-fold. Thus, they offer promising potential as sustainable alternatives to synthetic commercial fibers. Furthermore, our research provides valuable insights into the fundamental essence of fiber toughness and tensile strength, challenging the conventional notion that these properties are contradictory. These findings have significant implications for guiding the production of synthetic commercial fibers that simultaneously possess high strength and ultra-toughness.

INTRODUCTION

Wise investment in superior tools yields fruitful returns over time, underscoring the pivotal role of advanced materials in enhancing productivity and propelling the advancement of human civilization. For instance, the invention and widespread use of commercial synthetic fibers such as nylon and Kevlar have significantly contributed to the development of contemporary civilization.[1] However, these synthetic fibers, including nylon, have become a double-edged sword, as their increasing usage poses a threat to sustainable development due to the depletion of fossil energy resources and environmental pollution.[1] Therefore, there is an urgent need to develop green, environmentally friendly, sustainable alternatives with ultra-high strength and toughness to promote ecological civilization without compromising productivity. While significant advancements have been made in recent years in the field of polymer fiber science and technology, the exploration of truly high-strength and ultra-tough advanced fibers remains ongoing. Unfortunately, current theories suggest that the properties of tensile strength and toughness in engineering materials are mutually exclusive,[2–5] resulting in compromises in commercial synthetic fibers between the two properties.[2–4] For example, well-known fibers like nylon and Kevlar, both being polyamide fibers, exhibit a trade-off, with nylon possessing higher toughness, while Kevlar demonstrates superior

PROGRESS AND POTENTIAL

Lightweight materials with super strength and toughness are highly sought after. Spider silk, a sustainable material, meets these requirements but faces challenges in commercialization due to scientific understanding of its spinning mechanism, technical complexities in the process, and engineering hurdles in low-cost mass production. Here, drawing inspiration from nylon and Kevlar, we propose a theory on the nature of toughness and strength, unveiling the basic structure of silk fibers. Using these theories, we successfully produce the first "localized" full-length spider silk fiber via transgenic silkworms, showcasing high tensile strength (1,299 MPa) and exceptional toughness (319 MJ/m^3). This breakthrough overcomes scientific, technical, and engineering obstacles, paving the way for spider silk's commercialization as a sustainable substitute for synthetic fibers. Moreover, our theories provide essential guidance for developing super materials.

Please cite this article in press as: Mi et al., High-strength and ultra-tough whole spider silk fibers spun from transgenic silkworms, Matter (2023), https://doi.org/10.1016/j.matt.2023.08.013

tensile strength.[6–12] Thus, unraveling the underlying scientific challenge of combining fiber toughness and strength is crucial and unavoidable for the development of super materials that meet the growing industrial demands for high strength and ultra-toughness.

The field of biomimetics, drawing inspiration from nature, has led to the efficient development of advanced materials and tools.[13] Natural polyamide fibers like silkworm silk and spider silk, particularly the latter, have long served as sources of inspiration for materials scientists.[7,13–15] In fact, Jeffrey L. Yarger pointed out that nylon itself was inspired by silk fibers, both being polyamide fibers.[16] Spider silk exhibits higher tensile strength than nylon and greater toughness than Kevlar.[6,17–19] Therefore, silk fibers from silkworms and spiders, possessing both high strength and exceptional toughness (unlike what is observed in engineering materials, where toughness and strength tend to be mutually exclusive), can serve as excellent research materials for deciphering the essence of toughness and strength.[20–22] Silk mechanical properties are determined by the quaternary structure, which is influenced by both the primary structure and the spinning process. Within silkworm silk fibers, glycine (Gly) and alanine (Ala) amino acids account for over 75% of the protein composition.[23] The repetitive sequence (Gly-Ala-Gly-X)n forms the β-sheet crystalline regions in silkworm silk fibers. In spider silk, β-sheet crystalline regions are formed by GGX (X = A, Q, or Y), GX (X = Q, A, or R), and polyalanine sequences.[24–26] These repetitive sequences in silk fibers, whether derived from silkworms or spiders, play a crucial role in determining their strength and toughness by facilitating the formation of β-sheet crystalline regions. It is noteworthy that despite relying on weak non-covalent interactions, such as hydrogen bonds,[27] these β-sheet crystalline regions contribute significantly to the overall mechanical properties of silk fibers. Moreover, silkworm silk and spider silk align with the principles of sustainability and environmental friendliness, making them outstanding candidates to replace synthetic commercial fibers like nylon, thus promoting ecological civilization. However, achieving low-cost, large-scale production of mechanically robust fibers is crucial for their commercialization. However, silkworm silk, despite being the only animal protein fiber commercially produced on a large scale due to its low production cost, mostly restricts its application to the textile industry due to its limited mechanical performance. Spider silk, one of the strongest fibers, including commercial synthetic fibers, remains challenging to commercialize due to the cannibalistic nature of spiders, making large-scale silk production through rearing difficult. However, advancements in genetic engineering enable the expression of spider silk proteins via heterologous hosts and subsequent extrusion into spider silk *in vitro*.[27,28] The mechanical properties of both silk and spider silk are determined by their protein quaternary structures, which are influenced by both primary protein structure and spinning processes.[16] However, due to an incomplete understanding of the spinning mechanisms[17,29] and the intrinsic nature of silk fiber toughness and strength yet to be unraveled,[16] even the most advanced microfluidic spinning techniques fail to replicate the physicochemical environment required for natural silkworm silk and spider silk spinning.[30,31] Consequently, most synthetic spider silk fibers currently available exhibit inferior mechanical properties in one or more aspects compared with their natural counterparts.[16,32] Moreover, due to the inherent challenge of replicating the protective "cuticle layer" found in natural silk[33,34] and spider silk,[17,35–37] the maintenance duration of the mechanical properties in artificial spider silk and regenerated silk fibers is significantly shorter compared with their natural counterparts. In fact, in our laboratory, wet-spun spider silk experiences a significant decline in mechanical properties within a few weeks. This is another critical factor that impedes the commercialization of artificial spider

[1]College of Biological Science and Medical Engineering, Donghua University, Shanghai, China

[2]Biological Science Research Center, Southwest University, Chongqing, China

[3]Key Laboratory of Textile Science & Technology of Ministry of Education, College of Textiles, Donghua University, Shanghai, China

[4]State Key Laboratory of Silkworm Genome Biology, Southwest University, Chongqing, China

[5]Lead contact

*Correspondence: xiaqy@swu.edu.cn (Q.X.), mengqing@dhu.edu.cn (Q.M.)

https://doi.org/10.1016/j.matt.2023.08.013

Please cite this article in press as: Mi et al., High-strength and ultra-tough whole spider silk fibers spun from transgenic silkworms, Matter (2023), https://doi.org/10.1016/j.matt.2023.08.013

silk, a factor that is often overlooked by researchers. Therefore, addressing the aforementioned scientific and engineering challenges is essential for realizing silkworm silk or spider silk as alternatives to advanced commercial fibers like nylon and fostering the development of ecological civilization.

The silk glands of domestic silkworms and spider silk glands exhibit remarkably similar physicochemical environments.[38,39] Therefore, by leveraging the high-density cultivation of domestic silkworms for spider silk production, we can overcome the scientific challenges associated with the yet-to-be-fully-deciphered spinning mechanism of spider silk and the technical hurdles in developing spinning processes. This approach also enables us to address the engineering obstacles involved in achieving low-cost, large-scale production of spider silk.[40,41] Moreover, spider silk produced by domestic silkworms retains the cuticle layer, allowing it to maintain its mechanical properties over an extended period,[33,34] thereby facilitating the commercialization of spider silk fibers. However, even with the use of genetically modified domestic silkworms for spider silk production, the fundamental scientific question regarding the strength and toughness of silk fibers cannot be circumvented. This fundamental question has been a significant factor preventing previous studies utilizing genetically modified silkworms from surpassing the comprehensive mechanical performance of natural spider silk.[40–44] Only by unraveling the essence of strength and toughness and using it as guidance, through the "localization" of spider silk proteins within silkworm silk glands, can we enable the spider silk proteins to adapt to the silkworm glands. This approach will allow us to produce high-performance spider silk using domestic silkworms and achieve true commercialization with low-cost, large-scale production, leveraging genetically modified silkworms.

Here, drawing inspiration from the contrasting mechanical properties of nylon and Kevlar, both of which are polyamide fibers, we propose a theoretical framework that elucidates the fundamental factors determining fiber toughness and strength. Subsequently, employing a homology modeling approach, we introduce a novel minimal structural model for silk. This model is applicable for explaining and predicting the mechanical performance differences between silkworm silk and spider silk, both of which are polyamide fibers. Additionally, it guides the localization of spider silk proteins within domestic silkworm silk glands. Subsequently, we employed CRISPR-Cas9-mediated silk spinning in silkworms to successfully generate complete full-length spider silk fibers. This achievement serves as confirmation of our theory and yields spider silk fibers with both high strength and ultra-toughness. Scientific theories should not only possess testability but should also offer falsifiable predictions. Consequently, we confirm the validity of our theory by demonstrating its accurate predictions through the verification of phenomena from two distinct perspectives. This work resolves the scientific, technical, and engineering challenges that hinder the commercialization of high-performance spider silk. It holds the potential to replace commercial synthetic fibers such as nylon with spider silk, thereby promoting sustainable and environmentally friendly development within the realm of ecological civilization.

RESULTS

The fundamental factors determining fiber toughness and strength: Insights from nylon and Kevlar

The mechanical properties of polymers are closely related to their molecular structure, primarily determined by non-covalent interactions such as hydrogen bonding.[5,45,46] It was previously believed that the toughness of spider silk was attributed to its high cohesive energy density, resulting from a dense network of hydrogen

Please cite this article in press as: Mi et al., High-strength and ultra-tough whole spider silk fibers spun from transgenic silkworms, Matter (2023), https://doi.org/10.1016/j.matt.2023.08.013

bonds.[5,16,47] Cohesive energy refers to the energy required to separate 1 mol of a substance by breaking all intermolecular forces, primarily non-covalent interactions in the case of polymeric materials.[48] However, this theory fails to explain the significantly lower toughness observed in silkworm silk fibers, which possess a higher cohesive energy density than spider silk[49] (Table S1).

As mentioned earlier, nylon and Kevlar, both polyamide fibers, exhibit significant differences in toughness and tensile strength[6,7] (Table S2), indicating a potential trade-off between these properties.[2–5] This pronounced disparity provides a valuable opportunity to investigate the fundamental nature of fiber strength and toughness, inspiring our exploration into these attributes. Nylon and Kevlar demonstrate exceptional mechanical performance due to their high density of non-covalent interactions, including hydrogen bonding[50] (Figure S1). Similarly, spider silk, with its higher density of non-covalent interactions, particularly hydrogen bonding, exhibits greater toughness than Kevlar and higher tensile strength than nylon (Figure S1; Table S2). Additionally, polymer molecular weight is a critical parameter in developing fibers with high tensile strength and toughness.[51] Spider silk follows this trend, as its tensile strength and toughness increase with molecular weight (chain length).[7,52–54] Undoubtedly, these observations suggest a close correlation between non-covalent interactions, including hydrogen bonding, within fibers and their toughness and strength (Figure S1). However, the specific nature of this relationship and the apparent mutual exclusivity of tensile strength and toughness, both influenced by non-covalent interactions, remain intriguing questions.[2–5]

When fibers are subjected to stretching, the tensile force propagates along the fiber axis[55] and is transmitted through the molecular main chains. During the stage of elastic deformation, the relative positions of the molecules remain unchanged. At this point, the intramolecular non-covalent interactions within the fiber, referred to as "intramolecular static frictional force," and the intermolecular non-covalent interactions, known as "intermolecular static frictional force," collectively oppose the applied force. In the plastic deformation stage, there is a relative change in the positions of the molecules. Under the influence of the tensile force, the molecular chains slide relative to each other, leading to the repetitive breaking and formation of non-covalent bonds, such as hydrogen bonds, between molecules. This phenomenon, termed "intermolecular sliding frictional force," acts as the counteracting force to the applied force and enhances the overall dissipation of energy (i.e., toughness) within the fiber[16] (Videos S1, S2, and S3, where the red cylindrical objects represent non-covalent bonds such as hydrogen bonds and the blue represents the molecular backbone). In the realm of physics, work (W) is defined as the product of force (F) and distance (D), expressed as $W = FD$. Consequently, a greater intermolecular sliding frictional force and an increased relative sliding distance between molecules result in a higher amount of work performed by the intermolecular sliding frictional force to counteract the applied force, thus yielding a higher level of toughness. Therefore, we consider fiber toughness as a dynamic process (Videos S1, S2, and S3), with its essence encapsulated in the concept of average single-molecule intermolecular non-covalent bond energy density (ASM-INCBED). Increasing the length of the molecular chains within the fiber (i.e., the relative sliding distance between molecules, which determines the effect distance of the intermolecular sliding frictional force) and/or augmenting the non-covalent bond energy density between molecules (representing the intermolecular sliding frictional force) both contribute to an elevation in ASM-INCBED.

The term tensile strength characterizes a material's ability to withstand applied tensile force or stress. Therefore, the counteracting forces generated within the fiber to resist

Please cite this article in press as: Mi et al., High-strength and ultra-tough whole spider silk fibers spun from transgenic silkworms, Matter (2023), https://doi.org/10.1016/j.matt.2023.08.013

the applied force define the essence of tensile strength. We perceive the tensile strength of the fiber (during the plastic deformation stage) as a static moment in time, contingent upon the INCBED, specifically the corresponding intermolecular static frictional force at that particular moment. During the stretching of the fiber, relative sliding between molecules occurs, and a larger intermolecular static frictional force transforms into a larger intermolecular sliding frictional force. (An intriguing analogy to contemplate: consider toughness as the area enclosed by the stress-strain curve. If we envision tensile stress, or tensile strength, as a snapshot at a specific moment, it is dependent on the intermolecular static frictional force at that instant. If we view strain as the "time axis," as strain increases over time, the intermolecular static frictional force frame by frame transforms into the intermolecular sliding frictional force.) Consequently, under identical conditions of tensile strain, a higher tensile strength (tensile stress) corresponds to a greater level of toughness.

However, it is important to note that an excessive "intermolecular frictional force" beyond the critical value, which the covalent bonds within the molecular main chains of the material can withstand, hinders the relative sliding between molecules. This hindrance leads to the rupture of covalent bonds within the molecular chains during stretching, resulting in a material that possesses strength but exhibits brittleness. For example, Kevlar becomes strong yet brittle due to the presence of non-covalent bonds such as benzene rings and hydrogen bonds. These non-covalent bonds generate an intermolecular frictional force that exceeds the critical value that the molecular main chains of the polyamide fiber can bear. Consequently, the covalent bonds within the molecular chains break, contributing to its brittle nature (Figure S1; Video S2). On the other hand, nylon possesses a lower density of hydrogen bonds and other non-covalent bonds, which are significantly below the critical intermolecular frictional force that the molecular main chains of the polyamide fiber can tolerate. As a result, nylon exhibits considerable intermolecular sliding (higher tensile strain), leading to greater toughness. However, due to the lower intermolecular frictional force, nylon also possesses lower tensile strength (Figure S1; Video S1; Table S2).

Spider silk, with its optimal combination of hydrogen bonds and other non-covalent bonds, achieves an ideal density of intermolecular frictional forces. This unique balance between molecular interactions contributes to its high strength and exceptional toughness (Figure S1; Video S3). According to the INCBED and ASM-INCBED theories, enhancing intermolecular frictional forces before reaching the critical value allows for simultaneous improvement in both tensile strength and toughness. The key lies in maintaining intermolecular frictional forces slightly below the critical value that the covalent bonds within the material's molecular main chains can endure, enabling the material to achieve maximum toughness at the highest strength based on its properties. Exceeding the critical value of intermolecular frictional force results in a brittle material, thereby explaining the inherent contradiction between strength and toughness observed in previous studies.[2–5] Previous research has demonstrated that crosslinking spider silk proteins with formaldehyde leads to the formation of fibers that are strong yet brittle.[56] This phenomenon, where materials become strong but brittle due to covalent crosslinking, is commonly observed in the field of materials science.[4] The essence of this phenomenon lies in the fact that intermolecular covalent bonding increases the intermolecular frictional force beyond the critical value.

Structural model for the minimal basic unit of silkworm silk: Fib-H_{12}Fib-$L_{12}P25_2$ ($H_{12}L_{12}P25_2$)

The mechanical properties of protein fibers increase with the molecular weight of silk fibroin, as reported in previous studies.[52–54,57] However, silk fibers derived from the

Please cite this article in press as: Mi et al., High-strength and ultra-tough whole spider silk fibers spun from transgenic silkworms, Matter (2023), https://doi.org/10.1016/j.matt.2023.08.013

fibroin heavy chain (Fib-H) of silkworms, with a high molecular weight of up to 390 kDa, exhibit significantly inferior mechanical performance compared with spider silk, which has a smaller molecular weight (approximately 150 kDa[58] for the minor ampullate spidroin [MiSp]).[32,59] The presence of a substantial number of hydrogen bonds within β-sheet nanocrystals contributes to the enhancement of tensile strength in both silkworm silk and spider silk fibers.[16,32,49,60] Surprisingly, silkworm silk fibers with a higher proportion of β-sheet nanocrystals (49%–57%[61–63]) demonstrate lower tensile strength compared with naturally occurring spider silk, which possesses a lower β-sheet nanocrystal content (36%–46%[61,63]).[49] This suggests that the high content of β-sheet nanocrystals alone does not fully explain the underlying nature of strength, indicating the presence of other contributing factors. These observations may be attributed to structural differences between silkworm silk and spider silk, resulting in lower INCBED and ASM-INCBED in silkworm silk relative to spider silk. Therefore, there is an urgent need to unravel the structural characteristics of silkworm silk, aiming to localize spider silk proteins within the glands of transgenic silkworms, in order to obtain silk fibers with both ultra-high strength and ultra-toughness.

Silk fibers, found in both silkworms and spiders, consist of a hydrophilic N-terminal (NT) non-repetitive region, a hydrophobic repetitive region (R), and a hydrophilic C-terminal (CT) non-repetitive region.[38,64,65] The repetitive region is responsible for the formation of β-sheet nanocrystals, which greatly contribute to the mechanical properties of silk fibers.[29,52–54] Spiders achieve the ordered arrangement of the repetitive region and the formation of β-sheet nanocrystals through the dimerization of spider silk protein's NT and CT.[38,64–66] Consequently, the absence of NT and CT in spider silk proteins hinders proper assembly and silk formation.[64,67] Additionally, spider silk proteins can be stored at high concentrations in silk glands due to the formation of a liquid crystalline state through regular molecular pre-aggregation facilitated by NT and CT interactions.[17,66,68]

Previous studies have revealed that the NT region of Fib-H in silkworm silk adopts an anti-parallel homotetramer conformation[69] (Figure 1A). However, using the SWISS-MODEL protein structure homology modeling server, we discovered that the CT region of Fib-H forms short three-turn α-helices and exists as monomers (Figure 1B). This asymmetry in Fib-H's termini, unlike spider silk proteins,[66] raises questions about its ability to undergo regular pre-aggregation in silk glands and form a liquid crystalline state.[68] According to literature research, the CT region of Fib-H forms a covalent bond with the fibroin light chain (Fib-L) through intermolecular disulfide bonds, resulting in the formation of a single molecule (Figure 1C; monomeric structure of Fib-L from the AlphaFold[70] database, known for its accuracy comparable to experimental results). Therefore, we hypothesize that during the evolution of silkworms, the biological function of CT, similar to that of spider silk proteins,[66] might have been lost due to unknown reasons. However, to compensate for this loss, Fib-L evolved to serve as a substitute for CT, capable of covalently attaching to the short CT region of Fib-H. If our hypothesis is correct, Fib-L should theoretically also form an anti-parallel homotetramer. To validate this, we utilized the Swiss-Model server for homology modeling and confirmed that Fib-L can indeed form an anti-parallel homotetramer. Furthermore, we employed the MultiFOLD Server[71] to simulate the quaternary structure of Fib-L based on its primary sequence. The predicted results confirmed the formation of an anti-parallel homotetramer by Fib-L (Figure 1D). The quality of the quaternary structure model is high, with a per-residue local distance difference test (plDDT) score of 0.879 and a predicted template modeling (PTM) score of 0.859. This preliminary evidence supports our hypothesis

Please cite this article in press as: Mi et al., High-strength and ultra-tough whole spider silk fibers spun from transgenic silkworms, Matter (2023), https://doi.org/10.1016/j.matt.2023.08.013

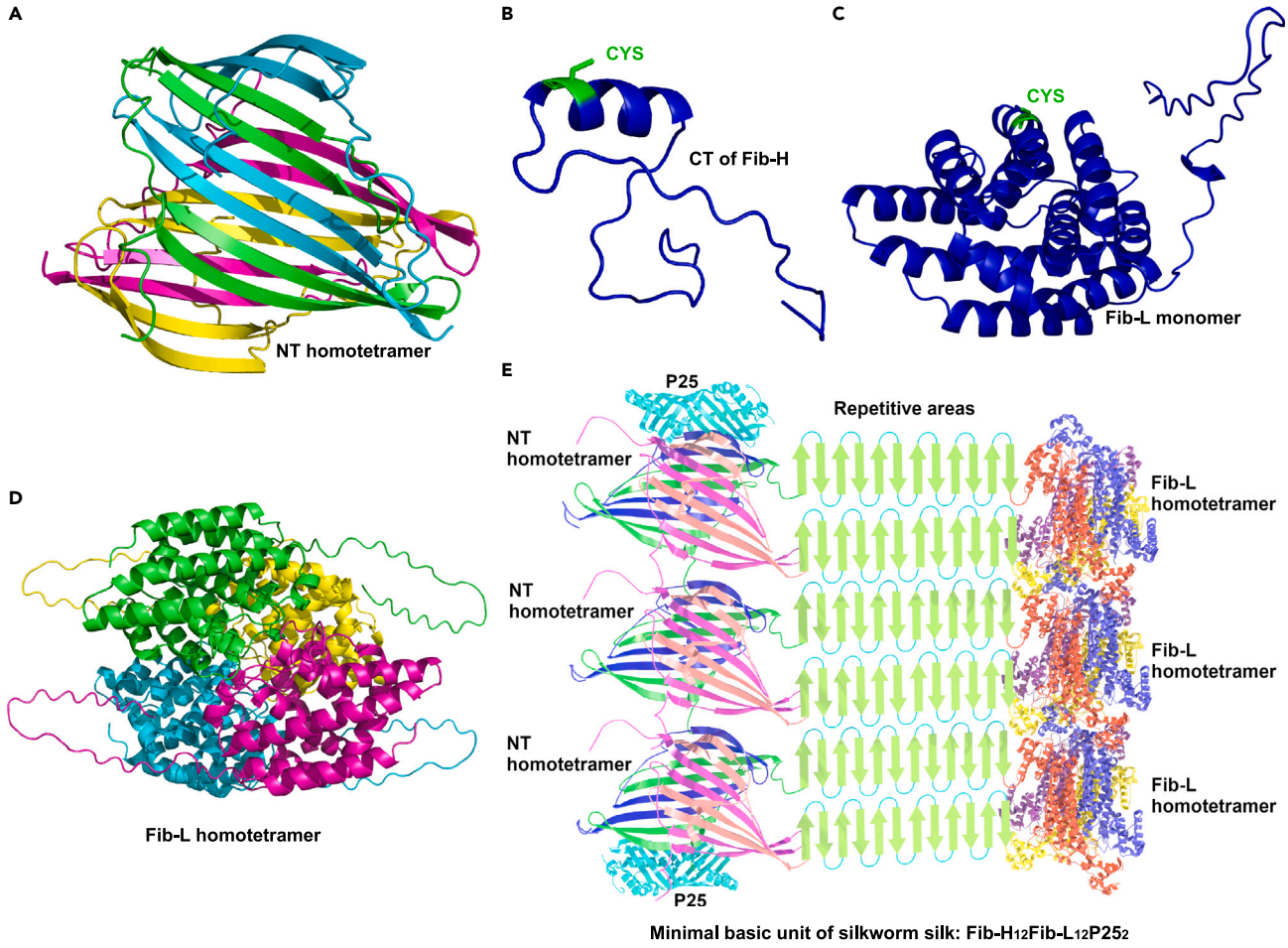

Figure 1. Diagram of the molecular models of silkworm silk

(A) Anti-parallel homotetrameric structure formed by the N-terminal (NT) region of Fib-H.

(B) Monomeric structure formed by the C-terminal (CT) region of Fib-H.

(C) Monomeric structure of Fib-L.

(D) Anti-parallel homotetrameric structure of Fib-L.

(E) The minimal fundamental unit of silk fiber: Fib-H_{12}Fib-$L_{12}P25_2$.

regarding the biological function of Fib-L as a surrogate for Fib-H's CT. Spider silk proteins lacking CT cannot form silk fibers, and if our hypothesis is correct, Fib-H lacking the "replacement CT" of Fib-L would also fail to spin properly. Supporting our conjecture, literature evidence shows that silkworms with Fib-L knocked out are unable to secrete silk proteins and develop into naked pupae.[72]

Why do higher β-sheet nanocrystals and a higher molecular weight in Fib-H result in lower tensile strength and toughness compared with spider silk? To address this question, it is crucial to examine the structural characteristics of the repetitive regions in Fib-H and spider silk proteins, as these regions significantly influence the mechanical properties of fibers.[29,52–54] One possible explanation for this disparity lies in the distinct biological functions of silkworm silk and spider silk. Silkworm silk primarily serves to protect the pupa from predators, requiring radial toughness in the silk filament (perpendicular to the plane of the cocoon) to resist pecking and tearing by birds. On the other hand, spider silk is primarily used by spiders for escape and capturing prey,[66] necessitating toughness along the fiber axis. Spider silk

Please cite this article in press as: Mi et al., High-strength and ultra-tough whole spider silk fibers spun from transgenic silkworms, Matter (2023), https://doi.org/10.1016/j.matt.2023.08.013

achieves a significant enhancement in its mechanical properties by forming CT homodimers with intermolecular disulfide bonds, leading to an increased length of the fiber's axial molecular chains.[57,64,66] Interestingly, the latest discovery reveals that spiders, in order to spin silk for escape or hunting purposes anytime and anywhere, have not evolved NT homodimers with intermolecular disulfide bonds similar to CT over hundreds of millions of years.[66] The repeated breaking and formation of hydrogen bonds and other non-covalent bonds, observed in materials like nylon and spider silk (Videos S1 and S3), contribute to their high toughness along the fiber axis. To achieve radial toughness in silkworm cocoons, a structural feature allowing repeated breaking and formation of hydrogen bonds and other non-covalent bonds in the radial direction was evolutionarily favored.

To gain insights into the structure of Fib-H's repetitive region, we conducted bioinformatics analysis. Our findings (Figures S2A–S2D) revealed that the repetitive region of Fib-H does not possess an unordered structure (Figure S2A), indicating that it folds into a regular conformation. The analysis consistently showed that the repetitive region predominantly adopts β-sheet structures, aligning with previous research findings (Figure S2B). Furthermore, our hydrophilicity analysis identified 11 regions of higher hydrophilicity in the repetitive region of Fib-H (Figure S2C), which may influence the folding orientation of the molecular chain. Additionally, we observed 11 peaks corresponding to the positions of hydrophilic sequences, indicating the presence of 11 loop turns of 180° in the repetitive region of Fib-H (Figure S2D), consistent with previous studies.[73] The structure of the repetitive region of the Fib-H from the bird-cherry ermine moth in the AlphaFold Protein Structure Database also demonstrates the formation of abundant intramolecular β-sheets (Figure S2E). These structural features may contribute to the radial toughness observed during fiber formation. Similarly, we analyzed these parameters for spider silk (MiSp) and found that the repetitive region of spider silk also forms β-sheet structures instead of being disordered (Figures S3A–S3D). However, the hydrophilicity of the repetitive region in spider silk is uniformly distributed and lacks the 11 high hydrophilicity peaks observed in Fib-H. Moreover, spider silk molecules do not exhibit the 11 β-turn peaks found in Fib-H. Therefore, it is evident that silkworm silk possesses 11 loop turns of 180°, absent in spider silk, which facilitate the formation of numerous intramolecular hydrogen bonds and other non-covalent bonds in the radial direction of the fiber. These findings support the initial hypothesis regarding the performance differences between silkworm silk and spider silk.

Previous studies have demonstrated that the molar ratio of Fib-H, Fib-L, and p25 in silkworm silk is 6:6:1, suggesting a minimal structural model of Fib-H_6Fib-L_6P25_1 ($H_6L_6P25_1$) for silk fibers.[74] However, our analysis reveals the formation of homotetramers at the N terminus of both Fib-H and Fib-L. Consequently, we propose a revised model for the fundamental unit of silkworm silk, consisting of three Fib-H4Fib-L4 hetero-oligomers interconnected by disulfide bonds,[74,75] along with the presence of two P25 glycoprotein molecules.[76,77] Specifically, Fib-H_{12}Fib-$L_{12}P25_2$ ($H_{12}L_{12}P25_2$) emerges as the minimal basic unit of silkworm silk (Figure 1E), thereby challenging the previously held notion of $H_6L_6P25_1$. Furthermore, the presence of 11 loop turns of 180° in silkworm silk results in the formation of numerous intramolecular hydrogen bonds and other non-covalent bonds in the radial direction (approximately 85% based on primary sequence calculations). When subjected to axial tension, this structural arrangement reduces the occurrence of intermolecular hydrogen bond formation and breakage, leading to lower INCBED and ASM-INCBED compared with spider silk (Video S4). Consequently, despite its higher molecular weight and a

Please cite this article in press as: Mi et al., High-strength and ultra-tough whole spider silk fibers spun from transgenic silkworms, Matter (2023), https://doi.org/10.1016/j.matt.2023.08.013

greater proportion of β-sheet nanocrystals, silkworm silk exhibits lower tensile strength and toughness along the fiber axis in comparison to spider silk.[49,52–54,57,61,63]

Validation of the INCBED and ASM-INCBED theories through CRISPR-Cas9-mediated production of full-length spider silk in silkworms

In this study, we employed CRISPR-Cas9 gene-editing technology to mediate the production of full-length spider silk (MiSp) in silkworms. Our objective was to validate the INCBED theory and the ASM-INCBED theory by comparing the strength and toughness of silkworm silk and spider silk, both produced through the same spinning process using silkworm silk glands. Referring to the minimal structural model of $H_{12}L_{12}P25_2$, we retained the CT and a portion of the NT of Fib-H to ensure successful secretion of the "localized" MiSp into the silkworm cocoon[72] (Figure 2A). Through our efforts, we successfully obtained transgenic silkworms expressing localized MiSp (Figures 2B and 2C). Subsequently, by examining the proteins in the spinning silk glands, we confirmed the expression of MiSp in the transgenic silkworms (Figure 2D). Our observations revealed an increase in the amino acids Val, Leu, His, and Arg and a decrease in Ser, providing support for the notion that transgenic silkworms can effectively secrete MiSp into the cocoon (Figures 2E and S4A). Notably, we found no discernible differences in the surface morphology of the silk fibers between wild-type, heterozygous, and homozygous silkworms (Figure 3A). This similarity likely stems from their common origin in silkworm silk glands. Furthermore, the content of β-sheet structures in silkworm silk fibers followed the order of wild type > homozygous > heterozygous (Figures 3B and S4B; Table S3). This finding aligns with the conclusion that silkworm silk exhibits a higher proportion of β-sheet nanocrystals compared with spider silk.[47,61–63] The reduced β-sheet content in heterozygous silkworm silk may be attributed to potential interference between the structures of Fib-H and MiSp. We observed an intriguing phenomenon in the regenerated silk protein solution where the β-sheet structures exhibited a decreasing trend in the order of wild type > heterozygous > homozygous, while conversely, the random coil structure showed an increasing trend following the same order (Figures S4C and S4D). This fascinating observation holds the potential to shed light on the silk spinning mechanisms employed by both silkworms and spiders.

According to the INCBED theory and the ASM-INCBED theory, the INCBED and ASM-INCBED of homozygous, heterozygous, and wild-type silk fibers should decrease sequentially (Figures 1E and S5A–S5C; Videos S3 and S4). By calculating data from group interaction modeling (GIM) in previous studies, we have confirmed that the results indeed align with this pattern.[49,78,79] The INCBED and ASM-INCBED of spider silk are indeed greater than those of silkworm silk (Table S1). Therefore, if the theory is correct, the breaking strength and toughness of fibers should decrease in the order of homozygous > heterozygous > wild type. The results of mechanical testing on the silk fibers align with our predictions, providing evidence for the validity of our proposed theories on the fundamental principles of toughness and strength inspired by nylon and Kevlar (INCBED theory and ASM-INCBED theory) (Figure 3C; Table S2). This challenges the previously held notion that toughness is determined by cohesive energy density.[47] Furthermore, this finding indirectly supports the accuracy of the $H_{12}L_{12}P25_2$ structural model. We believe that the utilization of the complete full-length MiSp sequence and the localization of MiSp within the transgenic silkworm silk glands, based on the $H_{12}L_{12}P25_2$ structural model, are crucial factors contributing to the achievement of high strength and toughness in silk fibers. This is because the mechanical properties of silk fibers depend on both the primary structure (complete full-length MiSp protein sequence) and the spinning process (specific MiSp localization adapted to the silkworm silk glands), which

Please cite this article in press as: Mi et al., High-strength and ultra-tough whole spider silk fibers spun from transgenic silkworms, Matter (2023), https://doi.org/10.1016/j.matt.2023.08.013

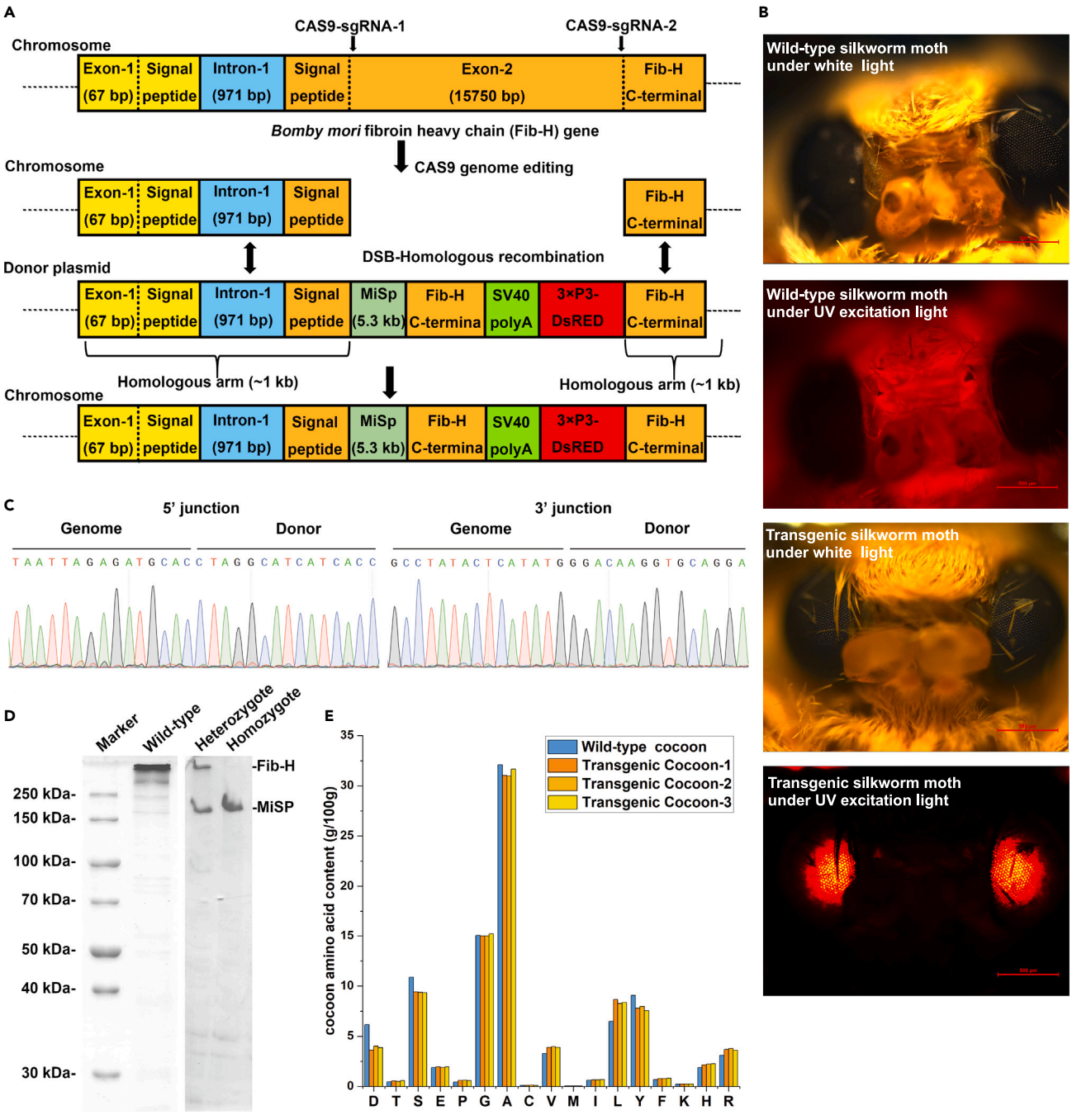

Figure 2. Replacement of Fib-H with the complete MiSp sequence using CRISPR-Cas9

(A) Schematic representation of CRISPR-Cas9 gene-editing technology.

(B) Fluorescent images of wild-type and transgenic silkworm moths under white and UV excitation light.

(C) DNA sequencing analysis of the 5′ and 3′ junctions in the genome of transgenic silkworms.

(D) Sodium dodecyl sulfate-polyacrylamide gel electrophoresis (SDS-PAGE) analysis of proteins in the silk glands of wild-type and transgenic silkworms.

(E) Quantification of amino acid contents in wild-type and transgenic homozygous silkworm cocoons.

collectively determine the quaternary structure. Consequently, we posit that these factors account for the suboptimal comprehensive mechanical performance observed in previous studies involving the production of spider silk through

Please cite this article in press as: Mi et al., High-strength and ultra-tough whole spider silk fibers spun from transgenic silkworms, Matter (2023), https://doi.org/10.1016/j.matt.2023.08.013

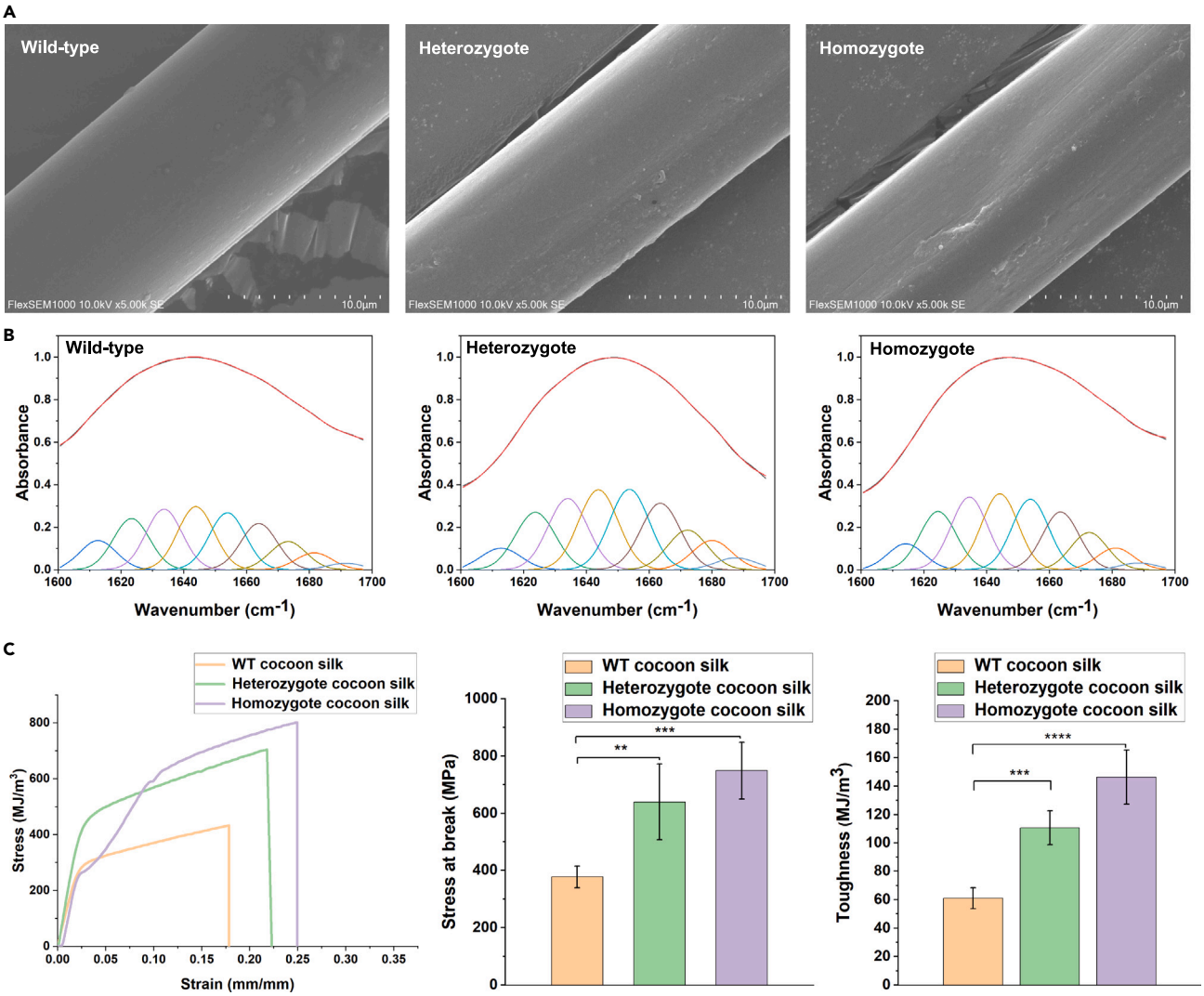

Figure 3. Conversion of intramolecular hydrogen bonds in silk to intermolecular hydrogen bonds significantly enhances the material's toughness

(A) Scanning electron microscopy (SEM) images displaying the morphologies of wild-type, heterozygous, and homozygous silk cocoons. Scale bars: 10 μm.

(B) Fourier transform infrared (FTIR) spectroscopy analysis revealing the corresponding secondary structures of the three silk variants. The calculation of the secondary structures is presented in Figure S4B.

(C) Stress-strain curves, tensile strength, and toughness measurements of the three silk fibers. The error bars represent standard deviations (n = 5). See also Figure S4 and Table S2.

transgenic silkworms,[40–44] where incomplete full-length spider silk sequences were employed and spider silk localization was not achieved.

It is worth noting that the tensile strength at the yield point of homozygous fibers is lower than that of wild-type silkworm silk fibers, but the breaking strength is significantly higher. Why does this occur? We will analyze and discuss this phenomenon in the next section.

Validation of the INCBED predictions through linear fit analysis of stress-strain behavior in silk fibers

A key characteristic of scientific theories is their predictive nature. Therefore, a good new theory should not only be supported by empirical evidence but should also

Please cite this article in press as: Mi et al., High-strength and ultra-tough whole spider silk fibers spun from transgenic silkworms, Matter (2023), https://doi.org/10.1016/j.matt.2023.08.013

propose testable predictions. According to the INCBED theory, increasing the INCBED of a material leads to an increase in its tensile strength. So, how can we increase the INCBED of silk fibers?

Cohesive energy is mainly composed of non-covalent bonds, such as hydrogen bonds, where the bond energy (E) increases as the distance (R) between atoms decreases. Non-covalent bonds are essentially governed by Coulombic forces, and thus the bond energy is inversely proportional to the square of the bond length.

$$E = \frac{\alpha}{R^2} \quad \text{(Equation 1)}$$

Here, α represents the system constant, R represents the intermolecular distance, and E represents the cohesive energy or bond energy of non-covalent bonds.

During the initial stretching stage of a fiber, the relative positions of the molecules remain unchanged, and therefore the number of non-covalent bonds in the fiber does not change. Additionally, in theory, the volume (V) of the fiber remains constant. However, as the fiber is stretched, its length (l) increases, resulting in a decrease in the cross-sectional area of the fiber and a reduction in the diameter (radius [r]) of the fiber in the radial direction. Consequently, the distance between molecules and atoms along the axis of the fiber decreases. According to Equation 1, this reduction in distance leads to an increase in the bond energy of non-covalent bonds.

$$V = \pi r^2 \times l \quad \text{(Equation 2)}$$

$$r = \sqrt{\frac{V}{\pi l}} \quad \text{(Equation 3)}$$

$$R = K r \quad \text{(Equation 4)}$$

$$E = \frac{\alpha}{R^2} = \frac{\alpha}{\left(K\sqrt{\frac{V}{\pi l}}\right)^2} = \frac{\alpha \pi l}{K^2 V} \quad \text{(Equation 5)}$$

Here, V represents the volume of the cylindrical silk fiber, r represents the radius of the fiber's cross-section, K represents the constant, and l represents the length of the fiber. By combining Equations 1, 3, and 4, we can derive Equation 5. As π, α, K, and V are constants, it follows from Equation 5 that the bond energy of non-covalent bonds is directly proportional to the length of the silk fiber. Thus, we can conclude that the INCBED of silk fibers is directly proportional to their length.

According to Equation 5, during the initial stage of stretching, the value of INCBED increases linearly with the length of the fiber. Therefore, to validate the predicted phenomenon of the INCBED theory, we conducted stretching experiments on three types of silk fibers and collected the initial strain and corresponding tensile strength at each point. Subsequently, we conducted a curve fitting analysis on the collected data points and observed a clear linear relationship between the two factors (Figure 4). This convincingly demonstrates the validity of the INCBED theory and verifies its predicted phenomenon. (In fact, from a reverse perspective, Equation 5 can also provide a fundamental explanation for the observed phenomenon of a proportional relationship between tensile strength and strain during the elastic deformation stage, as well as the nature of Young's modulus. However, as this is not the focus of this article, we will not delve into it further in this discussion.)

Please cite this article in press as: Mi et al., High-strength and ultra-tough whole spider silk fibers spun from transgenic silkworms, Matter (2023), https://doi.org/10.1016/j.matt.2023.08.013

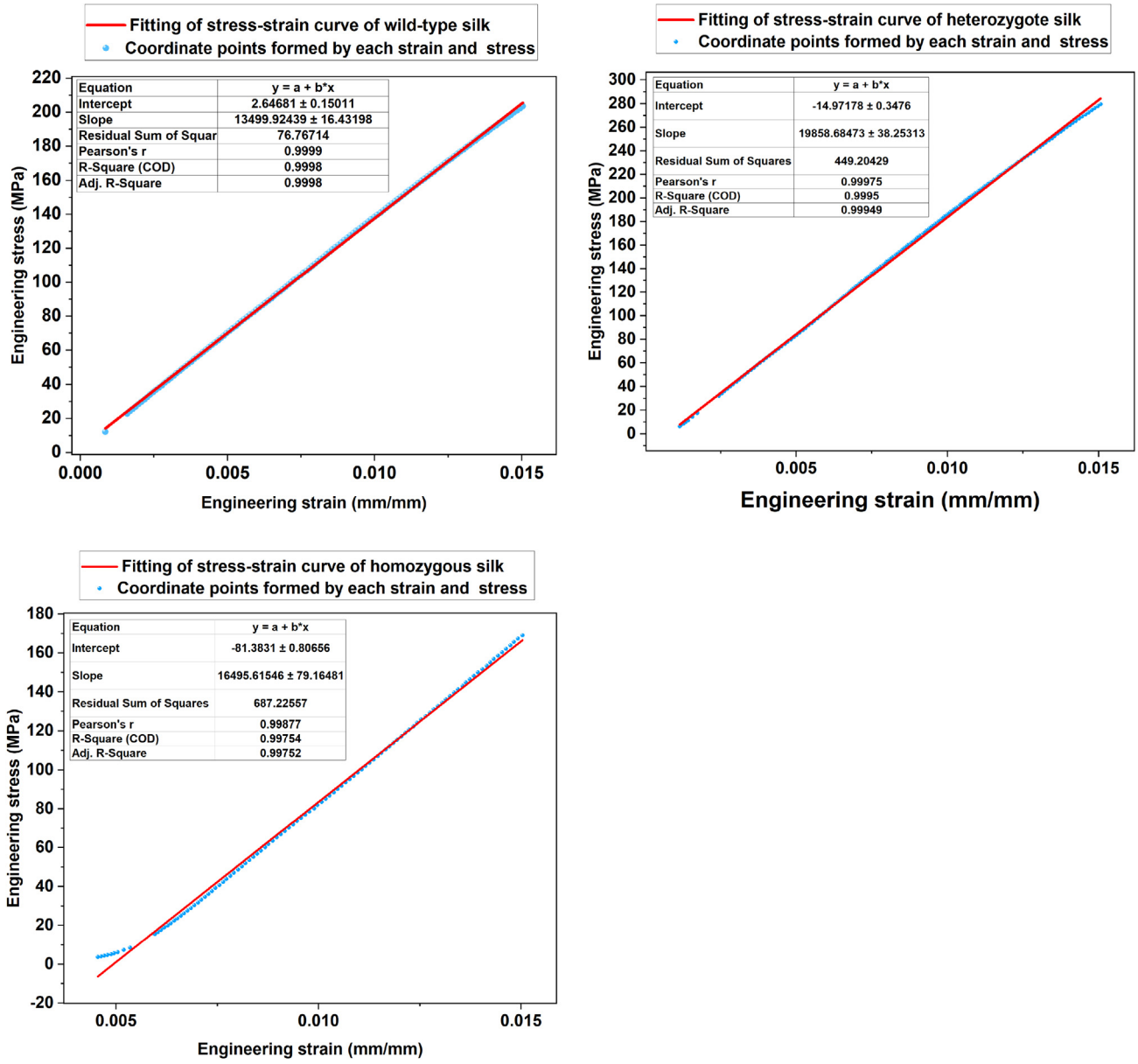

Figure 4. Stress-strain linear regression plots depicting the behavior of wild-type, heterozygous, and homozygous silkworm cocoon silk fibers prior to reaching the yield point

Next, we discuss the phenomenon mentioned in the previous section where the yield strength of pure homozygous silk fibers is lower than that of wild-type silk while the fracture strength is significantly higher. Tensile strength refers to the ability of a material to withstand tension or stress under a stretching load. Thus, the internal forces within the fiber that counteract the applied tension are essential to determine the material's tensile strength. During the initial stage of stretching, known as the elastic deformation stage, the molecules within the fiber do not experience relative sliding. In this stage, both intramolecular and intermolecular non-covalent bonds contribute as reactive forces against the applied tension. Therefore, the tensile strength in this stage depends on the collective strength of all the non-covalent bonds within the material, referred to as the total cohesive energy density. Silk

Please cite this article in press as: Mi et al., High-strength and ultra-tough whole spider silk fibers spun from transgenic silkworms, Matter (2023), https://doi.org/10.1016/j.matt.2023.08.013

exhibits a higher cohesive energy density compared with spider silk due to its larger molecular weight and a higher proportion of β-sheet nanocrystals (Table S1). Consequently, silk has a greater yield strength than pure homozygous spider silk fibers. In the plastic deformation stage, relative sliding between the molecules occurs, and the reactive forces against tension primarily arise from intermolecular frictional forces. The intermolecular frictional force, referred to as the INCBED, is greater in spider silk than in silk (Table S1; Videos S3 and S4), resulting in a higher fracture strength for spider silk. Additionally, during the plastic deformation stage, the fiber's quaternary structure undergoes changes. It is postulated that small loop structures may also exist in spider silk. When tension is transmitted along the main chain, these tensions may align the small loop structures in parallel to the fiber axis. Consequently, a portion of the intramolecular non-covalent bonds convert into intermolecular non-covalent bonds, thereby increasing the INCBED. Due to the presence of larger amino acid segments on both sides of the 180° turn in silk, the total strength of intramolecular non-covalent bonds, such as hydrogen bonds, is significant and less susceptible to complete straightening by external tensile forces. As a result, the proportion of intramolecular non-covalent bonds transforming into intermolecular ones during plastic deformation is smaller in silk compared with in spider silk. Hence, these combined factors contribute to the higher fracture strength observed in pure homozygous silk compared with silk.

Validation of INCBED and ASM-INCBED predictions through forced reeling: Enhancing the toughness and strength of silk fibers

The proportion of β-sheet nanocrystals in the structure contains a high density of non-covalent bonds, such as hydrogen bonds.[61,63] Consequently, increasing the proportion of β-sheet nanocrystals in silk fibers often leads to an elevation in INCBED and ASM-INCBED. Forced reeling of silkworms can enhance the β-sheet content in silk fibers, and higher reeling speeds result in greater β-sheet content.[80,81] According to the predictions of the INCBED and ASM-INCBED theories, augmenting the proportion of β-sheet nanocrystals in silk fibers can improve their tensile strength and toughness.

To validate the predicted phenomena of the INCBED and ASM-INCBED theories, we conducted forced reeling experiments on three types of silkworms. We observed a significant decrease in the diameter of wild-type silk fibers as the forced reeling speed increased (Figure 5A; Table S2). This finding aligns with previous research results.[59,80,81] As anticipated, forced reeling increased the proportion of β-sheets in silk fibers, and this proportion exhibited an upward trend with higher reeling speeds (Figures 5B and S4B). These results are consistent with earlier studies.[80,81] Consequently, higher reeling speeds, leading to a higher β-sheet content, contribute to increased INCBED and ASM-INCBED in silk fibers. As predicted by the INCBED and ASM-INCBED theories, this enhancement translates into improved toughness and strength. The mechanical performance tests support this observation (Figures 5C, S4E, and S4F; Table S2) and align with previous experimental findings,[59,80,82–84] further validating the accuracy of the INCBED and ASM-INCBED theories.

Faster forced reeling speeds have been shown to result in finer silk fibers[80,81,84] and higher β-sheet content, as well as increased molecular orientation.[80,81] Previous research has associated smaller fiber diameters with increased stress and toughness.[47] We speculate that this phenomenon can be attributed to the diminishing effect of shear forces from the fiber shell to the core (Figures S6 and S7). Thus, with finer fibers, shear forces can more effectively act on the silk fiber core, leading to improved strength and toughness.[47] However, the exact nature of this phenomenon

Please cite this article in press as: Mi et al., High-strength and ultra-tough whole spider silk fibers spun from transgenic silkworms, Matter (2023), https://doi.org/10.1016/j.matt.2023.08.013

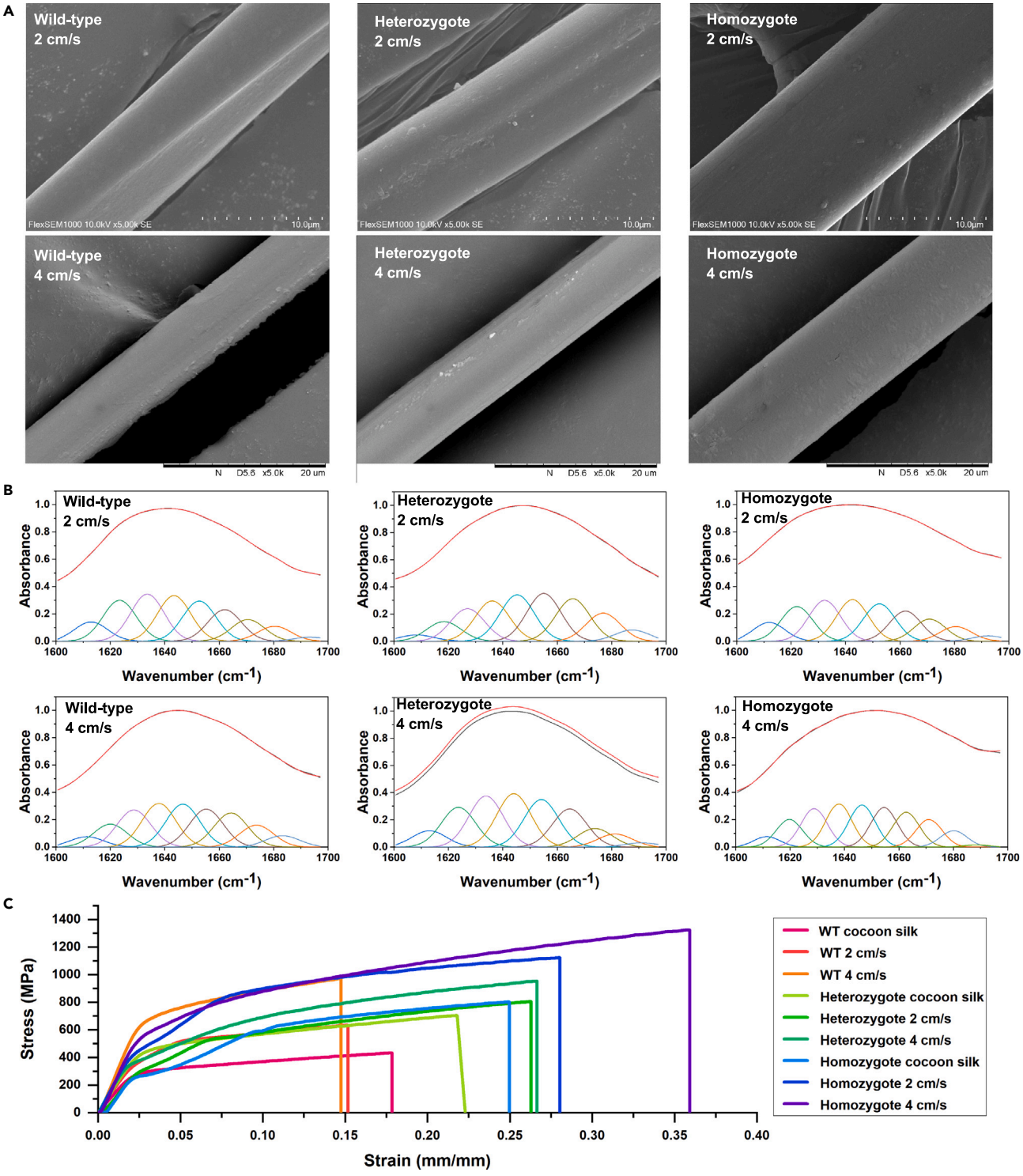

Figure 5. Forced reeled silk exhibited enhanced stress resistance and toughness

(A) SEM images of forced reeled silks. The scale bars for images with a speed of 2 cm/s are 10 μm, while for images with a speed of 4 cm/s, the scale bars are 20 μm.

(B) Determination of the secondary structure contents of forced reeled silks using FTIR spectroscopy. The calculation of secondary structures is presented in Figure S4B.

(C) Stress-strain curves of forced reeled silks. For corresponding column plots of tensile strength and toughness, refer to Figures S4E and S4F. See also Figure S4 and Table S2.

Please cite this article in press as: Mi et al., High-strength and ultra-tough whole spider silk fibers spun from transgenic silkworms, Matter (2023), https://doi.org/10.1016/j.matt.2023.08.013

has not been fully elucidated to date. In light of the INCBED and ASM-INCBED theories presented in this study, we seek to provide an explanation[47]: shear forces can increase the β-sheet content of silk fibers (i.e., increase the INCBED and ASM-INCBED of the fibers), albeit with a diminishing effect from the fiber shell to the core. Consequently, the distribution of β-sheet content in silk fibers can be inferred to be non-uniform, decreasing from the fiber shell to the core. If shear forces follow a uniform decreasing pattern, the toughness of silk fibers would increase by approximately 1.5 times for every halving of the fiber diameter. Additionally, shear forces can straighten loop structures within the molecules, converting some intramolecular non-covalent bonds into intermolecular ones, thereby enhancing the toughness and strength of the fiber. Furthermore, we conducted a fitting analysis of the initial tensile stress and strain during the stretching stage of the forced reeling fibers (data not shown) and found a proportional relationship similar to that shown in Figure 4. This further supports the validity of the INCBED theory.

DISCUSSION

Drawing inspiration from the mechanical performance disparities between nylon and Kevlar, which are both polyamide fibers, we have proposed theories regarding the fundamental nature of toughness and strength (INCBED theory and ASM-INCBED theory). Subsequently, employing bioinformatics analysis, we have introduced the latest model of silk's minimal structural unit ($H_{12}L_{12}P25_2$) with the aim of facilitating the integration of spider silk within silkworms, a process known as localization. By harnessing CRISPR-Cas9 gene-editing technology, we have successfully accomplished the complete substitution of Fib-H's intermediate repeat region with MiSp, thereby substantiating the INCBED theory and the ASM-INCBED theory. Additionally, we have validated two anticipated phenomena based on these theories, offering compelling evidence of their validity. Consequently, we have reached a significant milestone by obtaining the first genetically modified silkworm capable of spinning the whole spider silk. The resultant silk fibers exhibit remarkable characteristics, including high tensile strength (1,299 MPa) and extraordinary toughness (319 MJ/m^3). This groundbreaking achievement effectively resolves the scientific, technical, and engineering challenges that have hindered the commercialization of spider silk, positioning it as a viable alternative to commercially synthesized fibers like nylon and contributing to the advancement of ecological civilization.[7,14,16,17,47,85]

The INCBED theory and ASM-INCBED theory challenge the notion that toughness and strength in materials are mutually exclusive, contrary to previous beliefs.[2–5] These theories offer materials scientists confidence and theoretical guidance in the development of super materials. By optimizing the density of non-covalent bonds, such as hydrogen bonds, between polymer chains and by maximizing the "intermolecular friction," along with increasing chain length to allow for greater relative sliding distance (rupture strain), fibers with enhanced tensile strength and toughness can be achieved. This approach fully unleashes the mechanical potential of these materials by maximizing polymer chain length and the maximum intermolecular friction the backbone can withstand. For example, reinforcing the covalent bond strength in the molecular backbone of Kevlar, by replacing it with stronger covalent bonds, enables it to withstand the existing high intermolecular friction. By maintaining a strength of 3,600 MPa and allowing for the same relative sliding distance between molecules as nylon (tensile strain) (Video S5), the toughness of this material can reach up to 4.8 times that of nylon (Table S2), equivalent to 380 MJ/m^3. This surpasses the toughness of most natural and synthetic fibers,

Please cite this article in press as: Mi et al., High-strength and ultra-tough whole spider silk fibers spun from transgenic silkworms, Matter (2023), https://doi.org/10.1016/j.matt.2023.08.013

including *Caerostris darwini* major ampullate silk[86] (Table S2), successfully achieving the combination of ultra-high strength and ultra-toughness. Furthermore, it is worth noting that Equation 5 indicates that an increase in the system constant α can lead to a corresponding increase in both the INCBED and ASM-INCBED. This simultaneous augmentation contributes to the enhancement of the material's strength and toughness. Therefore, in line with the theoretical framework of this study, the manipulation of atomic-level atom arrangements and subsequent alterations to the system constant α offer a promising avenue for effectively bolstering the material's mechanical properties. Therefore, this study not only presents the potential to substitute synthetic commercial fibers such as nylon with spider silk, thereby promoting ecological development, but also provides theoretical guidance for the development of high-strength and ultra-tough materials across various structural domains. For instance, the INCBED theory and the ASM-INCBED theory can serve as guiding principles for the design of structurally robust materials capable of constructing space elevators, effectively combining ultra-high strength and ultra-toughness.[87] This has the promising prospect of significantly enhancing human productivity and propelling the advancement of civilization.

EXPERIMENTAL PROCEDURES

Resource availability

Lead contact

Please contact Dr. Junpeng Mi (junpengmi@mail.dhu.edu.cn) for any queries.

Materials availability

The target silk fibers can be generated according to the following experimental procedures. The materials generated in this study are available from the corresponding author upon request.

Data and code availability

All data reported in this paper will be shared by the lead contact upon request. This paper does not report original code.

Bioinformatics analysis

The IUPred3 server (https://iupred.elte.hu/) was utilized to predict the disordered regions in proteins using the IUPred3 long disorder tool. Additionally, the ANCHOR2 tool on the UPred3 server was employed to predict the binding regions between silk proteins derived from silkworm and spider silk. By simply copying and submitting the amino acid sequences of Fib-h and MiSp, the results can be calculated. Subsequently, we utilized several tools available on the Expasy server (https://web.expasy.org/protscale/) to analyze the predicted distribution of β-turns (using the β-turn scale/Deleage and Roux), the distribution of hydrophobic amino acids (using the Hydropath scale/Kyte and Doolittle), and the prediction of β-sheets (using the β-sheet scale/Levitt) in the Fib-H and MiSp proteins. By directly submitting the amino acid sequences of Fib-H and MiSp, we obtained instantaneous analysis results.

Protein structure analysis

The structure of the Fib-H NT anti-parallel homotetramer was directly obtained from the RCSB Protein Databank (PDB: 3UA0). However, utilizing the SWISS-MODEL protein structure homology modeling server, we observed that the CT of Fib-H can only adopt a short three-turn α-helix structure, existing as a monomer. The tertiary structure of the Fib-L monomer and the partially repeated region structure of Fib-H were acquired from the AlphaFold Protein Structure Database (https://alphafold.ebi.ac.uk/). Employing homology modeling through the SWISS-MODEL server, we discovered that Fib-L is indeed

Please cite this article in press as: Mi et al., High-strength and ultra-tough whole spider silk fibers spun from transgenic silkworms, Matter (2023), https://doi.org/10.1016/j.matt.2023.08.013

capable of forming an anti-parallel homotetramer (the highest-scoring homology model provided by SWISS-MODEL is PDB: 1AUW). To further validate our findings, we utilized the MultiFOLD server[71] to simulate the quaternary structure of Fib-L based on its primary sequence (https://www.reading.ac.uk/bioinf/MultiFOLD/MultiFOLD_form.html). By inputting the amino acid sequence of Fib-L and selecting A4 as the stoichiometry, the prediction revealed that Fib-L can form an anti-parallel homotetramer. The quality assessment of this quaternary structure model is remarkably high, with a plDDT score of 0.879 and a PTM score of 0.859 (scores above 0.5 typically indicate more complete and confident models, closely resembling the native structure).

Plasmid construction

Two single guide RNAs (sgRNAs) were designed to knock out Fib-H on the CCTop-CRISPR-Cas9 target online predictor website as follows: sgRNA1, 5′GATGCATCTC TAATTATTTC3′; sgRNA2, 5′TGTCCGTATCCCCTGCCAGC3′. The plasmids for expressing CAS9 protein and sgRNA in silkworms were provided by Prof. Qing-You Xia and were as follows: SgRNA1-F, 5′aaacGATGCATCTCTAATTATTTC3′; SgRNA1-R, 5′aagtGAAATAATTAGAGATGCATC3′; SgRNA2-F, 5′aaacTGTCCG-TATCCCCTGCCAGC3′; SgRNA2-R, 5′aagtGCTGGCAGGGGATACGGACA3′.

The above two primer pairs were annealed separately and ligated to sgRNA plasmids digested using Thermo Scientific BpiI (BbsI) restriction endonuclease. The pC131-N1-35S-YFP-MiSp plasmid was digested using BamHI and XhoI to obtain the complete MiSp full-length gene sequence. The complete MiSp was then ligated to the donor plasmid using a homologous recombinase. The pC131-N1-35S-YFP-MiSp plasmid was digested using BamHI and XhoI to obtain the complete MiSp full-length gene sequence. The complete MiSp was then ligated to the donor plasmid using a homologous recombinase. The above four plasmids were then extracted using an Endotoxin Free Plasmid Extraction Kit (TIANGEN Biotech [Beijing]) and configured to a working concentration of 300 ng/μL. The N4 silkworms and Nistari silkworms used in this study were provided by Prof. Wenkong Huang and Yongping Huang, respectively.

The high-fidelity enzymes used in this study were 2× Phanta Master Mix (Vazyme Biotech), 2×Fast Pfu Master Mix (Novoprotein, Shanghai, China), and Phusion DNA Polymerase (New England Biolabs). Clones were constructed using a NovoRec plus One step PCR Cloning Kit (Novoprotein/Sinobio) and a Ready-to-Use Seamless Cloning Kit (Sangon Biotech). We used TransStart Top Taq DNA Polymerase (TransGen Biotech) to identify the correct clones. Plasmid sequencing was performed at Biotech Bioengineering (Shanghai, China). We obtained endotoxin-free plasmids using an endotoxin-free plasmid macroextraction kit (DP117) (TIANGEN Biotech [Beijing]).

Silkworm transformation

Silkworms were fed fresh mulberry leaves and housed at 25°C and 80% relative humidity. Eggs were collected from the female moths within 6 h of laying and fixed on slides with glue. The eggs were then fumigated with formaldehyde for 5 min for disinfection. A 10 nL mix of CRISPR-Cas9 system plasmids was injected into each egg using Eppendorf's CellTram vario manual microinjector. The wounds in the eggs were sealed with instant adhesive and then placed in a sterile incubator at 25°C and 80% relative humidity for incubation. Silkworm moths expressing the red fluorescent protein in the eye were screened under an inverted fluorescence microscope (558 nm). Each positive moth was mated with a wild-type moth to produce the G2 generation. Homozygous transgenic silkworms were produced according to

Please cite this article in press as: Mi et al., High-strength and ultra-tough whole spider silk fibers spun from transgenic silkworms, Matter (2023), https://doi.org/10.1016/j.matt.2023.08.013

Mendel's law of inheritance. The genomic DNA of silkworms was extracted using the FastPure Blood/Cell/Tissue/Bacteria DNA Isolation Mini Kit (Vazyme Biotech).

Protein assay

Wild-type, heterozygous, and homozygous silkworms were selected for cocooning and dissected, and their silk glands were then removed. Proteins from the glands were extracted for sodium dodecyl sulfate-polyacrylamide gel electrophoresis experiments (Figure S8A). The cocoons of the three lines were then examined for amino acid contents using an amino acid analyzer (L-8900 Amino Acid Analyzer). Theoretical amino acid content calculations were performed for Fib-H and MiSp proteins by the ProtParam tool.

Scanning electron microscopy

The surface structures of silk fibers were observed using a scanning electron microscope (TM300 [Hitachi] and FLEXSEM1000 [Hitachi]).

Circular dichroism (CD) spectroscopy

The silkworm cocoons were boiled in a 0.05% sodium carbonate solution for 5 min to remove the sericin proteins. Subsequently, they were dissolved in an 8 M lithium bromide (LiBr) solution. The dissolved proteins were then dialyzed against pure water and diluted to a concentration of 0.1 mg/mL. CD spectra of the protein solutions were acquired at 20°C using a Chirascan 68 CD spectrophotometer, covering a wavelength range of 260–190 nm. The wavelength step size was set to 1 nm, and each measurement was repeated three times. The obtained CD spectra were subjected to secondary structure analysis of the proteins using the SELCON3 analysis program available on the online tool DichroWeb79 (http://dichroweb.cryst.bbk.ac.uk/html/home.shtml). Statistical analysis was performed using GraphPad Prism 9.

Fourier transform infrared (FTIR) spectroscopy

FTIR analysis was performed at room temperature with a Nicolet iN10MX FTIR instrument (Thermo Fisher Scientific, Waltham, MA, USA) within the wavenumber range of 4000 to 600 cm^{-1}; 128 scans were collected for each spectrum with a resolution of 4 cm^{-1}. The spectra were curve fitted using Gaussian peak shapes. Three replicate experiments were performed for each silk fiber. Secondary structure content was estimated by calculating the percentage of each secondary structure band. Bands at 1,605–1,639 and 1,690–1,695 cm^{-1} represented β-sheets; those at 1,640–1,649 cm^{-1} represented random coils; those at 1,650–1,658 cm^{-1} represented α-helices; and those at 1,659–1,689 cm^{-1} represented β-turns. Statistical analysis between β-sheets was then performed using Graphpad Prism 9.

Mechanical tests of silk fibers

Sericin was removed from wild-type, heterozygous, and homozygous silkworm cocoons, and the silk was glued to the sample holder.

The heads of silkworms from the three lines were collected during cocooning, fixed, and subjected to forced reeling at speeds of 2 or 4 cm/s (Figure S8B). The diameter of each silk fiber was measured using optical microscopy. Three positions were selected for each photograph, and the average diameter was measured and calculated using Phenom Image Viewer software. Each sample was adjusted to a length of 1 cm. Stress-strain curves of the silk fibers were obtained using an Agilent T150 UTM instrument (Agilent Technologies, Santa Clara, CA, USA) at 20°C and 50% humidity. The strain rate used in the tensile test was 1e−3 (1/s). Each sample was evaluated five times. Stress, strain, Young's

modulus, and toughness at break were calculated using Agilent NanoSuite software. Statistical analysis was done in Excel and Graphpad prism 9.

SUPPLEMENTAL INFORMATION

Supplemental information can be found online at https://doi.org/10.1016/j.matt.2023.08.013.

ACKNOWLEDGMENTS

We thank Prof. Bexiong Zhong of Zhejiang University, China, and Prof. Yongping Huang of the Chinese Academy of Sciences for the gift of silkworms. We thank Prof. Xiangqin Liu of Dalhousie University, Canada, for providing advice on experimental design. In addition, we would like to thank Dr. Xue Li, Dr. Minmin Zhang, Dr. Jie Zhang, Dr. Yihang Lu, M.S. Qingchun Shen, Dr. Shumeng Li, M.S. Xiu Li, M.S. Li Guo, and M.S. Yu Jiang from Donghua University, China, for their help with the experiments. Special thanks to Prof. Wengong Huang for his many gifts of silkworms. Financial support is provided by the following four grants: National Natural Science Foundation of China grant no. 31570721 (Q.M.); Key Projects of Science and Technology Commission of Shanghai Municipality grant no. 14521100700 (Q.M.); International Cooperation Projects of Science and Technology Commission of Shanghai Municipality grant no. 14520720200 (Q.M.); and Fundamental Research Funds for the Central Universities (Graduate Student Innovation Fund of Donghua University) grant no. CUSF-DH-D-2018067 (J.M.).

AUTHOR CONTRIBUTIONS

J.M., Y.Z., X.Z., and Q.M. developed the experimental design. J.M., S.M., Y.Z., S.X., Y.Y., Y.S., H.Z., S.W., and L.T. conducted the experiments and/or the materials characterization. Q.M., Q.X., and X.Z. supervised the research. J.M. contributed to the manuscript writing. Both INCBED and ASM INCBED theories were created by J.M. alone. Therefore, J.M.'s name is used to name these two theories: Junpeng Mi's INCBED (M-INCBED) theory and Junpeng Mi's ASM INCBED (M-ASM-INCBED) theory.

DECLARATION OF INTERESTS

The authors declare no competing interests.

INCLUSION AND DIVERSITY

We support inclusive, diverse, and equitable conduct of research.

Received: March 7, 2023
Revised: July 6, 2023
Accepted: August 22, 2023
Published: September 20, 2023

REFERENCES

1. Geyer, R., Jambeck, J.R., and Law, K.L. (2017). Production, use, and fate of all plastics ever made. Sci. Adv. *3*, e1700782. https://doi.org/10.1126/sciadv.1700782.

2. Ko, F.K., and Wan, L.Y. (2018). 6 - Engineering properties of spider silk. In Handbook of Properties of Textile and Technical Fibres, Second Edition, A.R. Bunsell, ed. (Woodhead Publishing), pp. 185–220. https://doi.org/10.1016/B978-0-08-101272-7.00006-7.

3. Song, P., Dai, J., Chen, G., Yu, Y., Fang, Z., Lei, W., Fu, S., Wang, H., and Chen, Z.-G. (2018). Bioinspired Design of Strong, Tough, and Thermally Stable Polymeric Materials via Nanoconfinement. ACS Nano *12*, 9266–9278. https://doi.org/10.1021/acsnano.8b04002.

4. Ritchie, R.O. (2011). The conflicts between strength and toughness. Nat. Mater. *10*, 817–822. https://doi.org/10.1038/nmat3115.

5. Li, Z., Zhu, Y.L., Niu, W., Yang, X., Jiang, Z., Lu, Z.Y., Liu, X., and Sun, J. (2021). Healable and Recyclable Elastomers with Record-High Mechanical Robustness, Unprecedented Crack Tolerance, and Superhigh Elastic Restorability. Adv. Mater. *33*, e2101498. https://doi.org/10.1002/adma.202101498.

6. Heim, M., Keerl, D., and Scheibel, T. (2009). Spider silk: from soluble protein to extraordinary fiber. Angew. Chem., Int. Ed.

Engl. *48*, 3584–3596. https://doi.org/10.1002/anie.200803341.

7. Li, J., Li, S., Huang, J., Khan, A.Q., An, B., Zhou, X., Liu, Z., and Zhu, M. (2022). Spider Silk-Inspired Artificial Fibers. Adv. Sci. *9*, e2103965. https://doi.org/10.1002/advs.202103965.

8. Roenbeck, M.R., Sandoz-Rosado, E.J., Cline, J., Wu, V., Moy, P., Afshari, M., Reichert, D., Lustig, S.R., and Strawhecker, K.E. (2017). Probing the internal structures of Kevlar® fibers and their impacts on mechanical performance. Polymer *128*, 200–210. https://doi.org/10.1016/j.polymer.2017.09.039.

9. Averett, R., Realff, M., Michielsen, S., and Neu, R. (2006). Mechanical behavior of nylon 66 fibers under monotonic and cyclic loading. Compos. Sci. Technol. *66*, 1671–1681. https://doi.org/10.1016/j.compscitech.2005.11.037.

10. Ebewele, R.O. (2000). Polymer Science and Technology (CRC press).

11. Halary, J.L., Laupretre, F., and Monnerie, L. (2011). Polymer Materials: Macroscopic Properties and Molecular Interpretations (Wiley).

12. Stevens, M.P. (1999). Polymer Chemistry: An Introduction (Oxford University Press).

13. Jung, D., Lee, J., Park, T.Y., Yang, Y.J., and Cha, H.J. (2021). Diverse silk and silk-like proteins derived from terrestrial and marine organisms and their applications. Acta Biomater. *136*, 56–71. https://doi.org/10.1016/j.actbio.2021.09.028.

14. Montero de Espinosa, L., Meesorn, W., Moatsou, D., and Weder, C. (2017). Bioinspired Polymer Systems with Stimuli-Responsive Mechanical Properties. Chem. Rev. *117*, 12851–12892. https://doi.org/10.1021/acs.chemrev.7b00168.

15. Hou, W., Wang, J., and Lv, J.a. (2023). Bioinspired Liquid Crystalline Spinning Enables Scalable Fabrication of High-Performing Fibrous Artificial Muscles. Adv. Mater. *35*, 2211800. https://doi.org/10.1002/adma.202211800.

16. Yarger, J.L., Cherry, B.R., and van der Vaart, A. (2018). Uncovering the structure–function relationship in spider silk. Nat. Rev. Mater. *3*, 18008. https://doi.org/10.1038/natrevmats.2018.8.

17. Vollrath, F., and Knight, D.P. (2001). Liquid crystalline spinning of spider silk. Nature *410*, 541–548. https://doi.org/10.1038/35069000.

18. Swanson, B.O., Blackledge, T.A., Summers, A.P., and Hayashi, C.Y. (2006). Spider dragline silk: correlated and mosaic evolution in high-performance biological materials. Evolution *60*, 2539–2551.

19. Blackledge, T.A., and Hayashi, C.Y. (2006). Silken toolkits: biomechanics of silk fibers spun by the orb web spider Argiope argentata (Fabricius 1775). J. Exp. Biol. *209*, 2452–2461. https://doi.org/10.1242/jeb.02275.

20. Ackbarow, T., and Buehler, M.J. (2009). Alpha-helical protein domains unify strength and robustness through hierarchical nanostructures. Nanotechnology *20*, 075103. https://doi.org/10.1088/0957-4484/20/7/075103.

21. Guo, K., and Buehler, M.J. (2019). Nature's Way: Hierarchical Strengthening through Weakness. Matter *1*, 302–303. https://doi.org/10.1016/j.matt.2019.07.011.

22. Nova, A., Keten, S., Pugno, N.M., Redaelli, A., and Buehler, M.J. (2010). Molecular and Nanostructural Mechanisms of Deformation, Strength and Toughness of Spider Silk Fibrils. Nano Lett. *10*, 2626–2634. https://doi.org/10.1021/nl101341w.

23. Mori, H., and Tsukada, M. (2000). New silk protein: modification of silk protein by gene engineering for production of biomaterials. J. Biotechnol. *74*, 95–103. https://doi.org/10.1016/S1389-0352(00)00004-0.

24. Wong Po Foo, C., and Kaplan, D.L. (2002). Genetic engineering of fibrous proteins: spider dragline silk and collagen. Adv. Drug Deliv. Rev. *54*, 1131–1143.

25. Hu, X., Vasanthavada, K., Kohler, K., McNary, S., Moore, A.M.F., and Vierra, C.A. (2006). Molecular mechanisms of spider silk. Cell. Mol. Life Sci. *63*, 1986–1999. https://doi.org/10.1007/s00018-006-6090-y.

26. Kuwana, Y., Sezutsu, H., Nakajima, K.i., Tamada, Y., and Kojima, K. (2014). High-Toughness Silk Produced by a Transgenic Silkworm Expressing Spider (Araneus ventricosus) Dragline Silk Protein. PLoS One *9*, e105325. https://doi.org/10.1371/journal.pone.0105325.

27. Ramezaniaghdam, M., Nahdi, N.D., and Reski, R. (2022). Recombinant Spider Silk: Promises and Bottlenecks. Front. Bioeng. Biotechnol. *10*, 835637. https://doi.org/10.3389/fbioe.2022.835637.

28. Zheng, K., and Ling, S. (2019). De Novo Design of Recombinant Spider Silk Proteins for Material Applications. Biotechnol. J. *14*, e1700753. https://doi.org/10.1002/biot.201700753.

29. Jin, H.J., and Kaplan, D.L. (2003). Mechanism of silk processing in insects and spiders. Nature *424*, 1057–1061. https://doi.org/10.1038/nature01809.

30. Wu, R., Bae, J., Jeon, H., and Kim, T. (2022). Spider-inspired regenerated silk fibroin fiber actuator via microfluidic spinning. Chem. Eng. J. *444*, 136556. https://doi.org/10.1016/j.cej.2022.136556.

31. Rising, A., and Johansson, J. (2015). Toward spinning artificial spider silk. Nat. Chem. Biol. *11*, 309–315. https://doi.org/10.1038/nchembio.1789.

32. Wang, J., Fan, T., Li, X., Hu, X., Huang, W., Yuan, W., and Lin, Z. (2022). Artificial superstrong silkworm silk surpasses natural spider silks. Matter *5*, 4396–4406. https://doi.org/10.1016/j.matt.2022.08.028.

33. Sarkar, A., Connor, A.J., Koffas, M., and Zha, R.H. (2019). Chemical Synthesis of Silk-Mimetic Polymers. Materials *12*, 4086. https://doi.org/10.3390/ma12244086.

34. Wöltje, M., and Böbel, M. (2017). 12 - Natural biodegradable medical polymers: Silk. In Science and Principles of Biodegradable and Bioresorbable Medical Polymers, X. Zhang, ed. (Woodhead Publishing)), pp. 351–376. https://doi.org/10.1016/B978-0-08-100372-5.00012-X.

35. Heim, M., Römer, L., and Scheibel, T. (2010). Hierarchical structures made of proteins. The complex architecture of spider webs and their constituent silk proteins. Chem. Soc. Rev. *39*, 156–164. https://doi.org/10.1039/b813273a.

36. Malay, A.D., Craig, H.C., Chen, J., Oktaviani, N.A., and Numata, K. (2022). Complexity of Spider Dragline Silk. Biomacromolecules *23*, 1827–1840. https://doi.org/10.1021/acs.biomac.1c01682.

37. Sponner, A., Vater, W., Monajembashi, S., Unger, E., Grosse, F., and Weisshart, K. (2007). Composition and hierarchical organisation of a spider silk. PLoS One *2*, e998. https://doi.org/10.1371/journal.pone.0000998.

38. Andersson, M., Chen, G., Otikovs, M., Landreh, M., Nordling, K., Kronqvist, N., Westermark, P., Jörnvall, H., Knight, S., Ridderstråle, Y., et al. (2014). Carbonic anhydrase generates CO2 and H+ that drive spider silk formation via opposite effects on the terminal domains. PLoS Biol. *12*, e1001921. https://doi.org/10.1371/journal.pbio.1001921.

39. Andersson, M., Johansson, J., and Rising, A. (2016). Silk Spinning in Silkworms and Spiders. Int. J. Mol. Sci. *17*, 1290. https://doi.org/10.3390/ijms17081290.

40. Teulé, F., Miao, Y.-G., Sohn, B.-H., Kim, Y.-S., Hull, J.J., Fraser, M.J., Lewis, R.V., and Jarvis, D.L. (2012). Silkworms transformed with chimeric silkworm/spider silk genes spin composite silk fibers with improved mechanical properties. Proc. Natl. Acad. Sci. USA *109*, 923–928. https://doi.org/10.1073/pnas.1109420109.

41. Xu, J., Dong, Q., Yu, Y., Niu, B., Ji, D., Li, M., Huang, Y., Chen, X., and Tan, A. (2018). Mass spider silk production through targeted gene replacement in Bombyx mori. Proc. Natl. Acad. Sci. USA *115*, 8757–8762. https://doi.org/10.1073/pnas.1806805115.

42. Tang, X., Ye, X., Wang, X., Zhao, S., Wu, M., Ruan, J., and Zhong, B. (2021). High mechanical property silk produced by transgenic silkworms expressing the spidroins PySp1 and ASG1. Sci. Rep. *11*, 20980. https://doi.org/10.1038/s41598-021-00029-8.

43. Zhang, X., Xia, L., Day, B.A., Harris, T.I., Oliveira, P., Knittel, C., Licon, A.L., Gong, C., Dion, G., Lewis, R.V., and Jones, J.A. (2019). CRISPR/Cas9 Initiated Transgenic Silkworms as a Natural Spinner of Spider Silk. Biomacromolecules *20*, 2252–2264. https://doi.org/10.1021/acs.biomac.9b00193.

44. Wen, H., Lan, X., Zhang, Y., Zhao, T., Wang, Y., Kajiura, Z., and Nakagaki, M. (2010). Transgenic silkworms (Bombyx mori) produce recombinant spider dragline silk in cocoons. Mol. Biol. Rep. *37*, 1815–1821. https://doi.org/10.1007/s11033-009-9615-2.

45. Lehn, J.-M. (1993). Supramolecular Chemistry. Science *260*, 1762–1763. https://doi.org/10.1126/science.8511582.

46. Prins, L.J., Reinhoudt, D.N., and Timmerman, P. (2001). Noncovalent Synthesis Using Hydrogen Bonding. Angew. Chem., Int. Ed. Engl. *40*,

2382–2426. https://doi.org/10.1002/1521-3773(20010702)40:13<2382::aid-anie2382>3.0.co;2-g.

47. Porter, D., Guan, J., and Vollrath, F. (2013). Spider silk: super material or thin fibre? Adv. Mater. *25*, 1275–1279. https://doi.org/10.1002/adma.201204158.

48. van Krevelen, D.W., and te Nijenhuis, K. (2009). Properties of Polymers: Their Correlation with Chemical Structure; Their Numerical Estimation and Prediction from Additive Group Contributions (Elsevier Science).

49. Guan, J., Wang, Y., Mortimer, B., Holland, C., Shao, Z., Porter, D., and Vollrath, F. (2016). Glass transitions in native silk fibres studied by dynamic mechanical thermal analysis. Soft Matter *12*, 5926–5936. https://doi.org/10.1039/c6sm00019c.

50. Appel, E.A., del Barrio, J., Loh, X.J., and Scherman, O.A. (2012). Supramolecular polymeric hydrogels. Chem. Soc. Rev. *41*, 6195–6214.

51. Volokhina, A.V. (2002). Effect of the Molecular Weight of Fibre-Forming Polymers on the Mechanical Properties of Polymer Fibres (Review). Fibre Chem. *34*, 1–9. https://doi.org/10.1023/A:1015564704979.

52. Xia, X.X., Qian, Z.G., Ki, C.S., Park, Y.H., Kaplan, D.L., and Lee, S.Y. (2010). Native-sized recombinant spider silk protein produced in metabolically engineered Escherichia coli results in a strong fiber. P Natl Acad Sci USA *107*, 14059–14063. https://doi.org/10.1073/pnas.1003366107.

53. Bowen, C.H., Dai, B., Sargent, C.J., Bai, W., Ladiwala, P., Feng, H., Huang, W., Kaplan, D.L., Galazka, J.M., and Zhang, F. (2018). Recombinant Spidroins Fully Replicate Primary Mechanical Properties of Natural Spider Silk. Biomacromolecules *19*, 3853–3860. https://doi.org/10.1021/acs.biomac.8b00980.

54. Heidebrecht, A., Eisoldt, L., Diehl, J., Schmidt, A., Geffers, M., Lang, G., and Scheibel, T. (2015). Biomimetic fibers made of recombinant spidroins with the same toughness as natural spider silk. Adv. Mater. *27*, 2189–2194. https://doi.org/10.1002/adma.201404234.

55. Xiao, S., Stacklies, W., Cetinkaya, M., Markert, B., and Gräter, F. (2009). Mechanical Response of Silk Crystalline Units from Force-Distribution Analysis. Biophys. J. *96*, 3997–4005. https://doi.org/10.1016/j.bpj.2009.02.052.

56. Zhu, H., Sun, Y., Yi, T., Wang, S., Mi, J., and Meng, Q. (2020). Tough synthetic spider-silk fibers obtained by titanium dioxide incorporation and formaldehyde cross-linking in a simple wet-spinning process. Biochimie *175*, 77–84. https://doi.org/10.1016/j.biochi.2020.05.003.

57. Lin, Z., Deng, Q., Liu, X.Y., and Yang, D. (2013). Engineered large spider eggcase silk protein for strong artificial fibers. Adv. Mater. *25*, 1216–1220. https://doi.org/10.1002/adma.201204357.

58. Chen, G., Liu, X., Zhang, Y., Lin, S., Yang, Z., Johansson, J., Rising, A., and Meng, Q. (2012). Full-length minor ampullate spidroin gene sequence. PLoS One *7*, e52293. https://doi.org/10.1371/journal.pone.0052293.

59. Shao, Z., and Vollrath, F. (2002). Surprising strength of silkworm silk. Nature *418*, 741. https://doi.org/10.1038/418741a.

60. Keten, S., Xu, Z., Ihle, B., and Buehler, M.J. (2010). Nanoconfinement controls stiffness, strength and mechanical toughness of β-sheet crystals in silk. Nat. Mater. *9*, 359–367. https://doi.org/10.1038/nmat2704.

61. Lefèvre, T., Rousseau, M.-E., and Pézolet, M. (2007). Protein Secondary Structure and Orientation in Silk as Revealed by Raman Spectromicroscopy. Biophys. J. *92*, 2885–2895. https://doi.org/10.1529/biophysj.106.100339.

62. Asakura, T., Yao, J., Yamane, T., Umemura, K., and Ulrich, A.S. (2002). Heterogeneous Structure of Silk Fibers from Bombyx mori Resolved by 13C Solid-State NMR Spectroscopy. J. Am. Chem. Soc. *124*, 8794–8795. https://doi.org/10.1021/ja020244e.

63. Paquet-Mercier, F., Lefèvre, T., Auger, M., Pézolet, M., and Paquet-Mercier, F. (2013). Evidence by infrared spectroscopy of the presence of two types of β-sheets in major ampullate spider silk and silkworm silk. Soft Matter *9*, 208–215. https://doi.org/10.1039/C2SM26657A.

64. Hagn, F., Eisoldt, L., Hardy, J.G., Vendrely, C., Coles, M., Scheibel, T., and Kessler, H. (2010). A conserved spider silk domain acts as a molecular switch that controls fibre assembly. Nature *465*, 239–242. https://doi.org/10.1038/nature08936.

65. Zhou, C.Z., Confalonieri, F., Medina, N., Zivanovic, Y., Esnault, C., Yang, T., Jacquet, M., Janin, J., Duguet, M., Perasso, R., and Li, Z.G. (2000). Fine organization of Bombyx mori fibroin heavy chain gene. Nucleic Acids Res. *28*, 2413–2419. https://doi.org/10.1093/nar/28.12.2413.

66. Mi, J., Zhou, X., Sun, R., and Han, J. (2023). Disabling spidroin N-terminal homologs' reverse reaction unveils why its intermolecular disulfide bonds have not evolved for 380 million years. Int. J. Biol. Macromol. *249*, 125974. https://doi.org/10.1016/j.ijbiomac.2023.125974.

67. Collin, M.A., Clarke, T.H., 3rd, Ayoub, N.A., and Hayashi, C.Y. (2018). Genomic perspectives of spider silk genes through target capture sequencing: Conservation of stabilization mechanisms and homology-based structural models of spidroin terminal regions. Int. J. Biol. Macromol. *113*, 829–840. https://doi.org/10.1016/j.ijbiomac.2018.02.032.

68. Kerkam, K., Viney, C., Kaplan, D., and Lombardi, S. (1991). Liquid crystallinity of natural silk secretions. Nature *349*, 596–598. https://doi.org/10.1038/349596a0.

69. He, Y.-X., Zhang, N.-N., Li, W.-F., Jia, N., Chen, B.-Y., Zhou, K., Zhang, J., Chen, Y., and Zhou, C.-Z. (2012). N-Terminal Domain of Bombyx mori Fibroin Mediates the Assembly of Silk in Response to pH Decrease. J. Mol. Biol. *418*, 197–207. https://doi.org/10.1016/j.jmb.2012.02.040.

70. Jumper, J., Evans, R., Pritzel, A., Green, T., Figurnov, M., Ronneberger, O., Tunyasuvunakool, K., Bates, R., Žídek, A., Potapenko, A., et al. (2021). Highly accurate protein structure prediction with AlphaFold. Nature *596*, 583–589. https://doi.org/10.1038/s41586-021-03819-2.

71. McGuffin, L.J., Edmunds, N.S., Genc, A.G., Alharbi, S.M.A., Salehe, B.R., and Adiyaman, R. (2023). Prediction of protein structures, functions and interactions using the IntFOLD7, MultiFOLD and ModFOLDdock servers. Nucleic Acids Res. *51*, W274–W280. https://doi.org/10.1093/nar/gkad297.

72. Ye, X., Tang, X., Zhao, S., Ruan, J., Wu, M., Wang, X., Li, H., and Zhong, B. (2021). Mechanism of the growth and development of the posterior silk gland and silk secretion revealed by mutation of the fibroin light chain in silkworm. Int. J. Biol. Macromol. *188*, 375–384. https://doi.org/10.1016/j.ijbiomac.2021.08.009.

73. Ha, S.W., Gracz, H.S., Tonelli, A.E., and Hudson, S.M. (2005). Structural study of irregular amino acid sequences in the heavy chain of Bombyx mori silk fibroin. Biomacromolecules *6*, 2563–2569. https://doi.org/10.1021/bm050294m.

74. Inoue, S., Tanaka, K., Arisaka, F., Kimura, S., Ohtomo, K., and Mizuno, S. (2000). Silk fibroin of Bombyx mori is secreted, assembling a high molecular mass elementary unit consisting of H-chain, L-chain, and P25, with a 6:6:1 molar ratio. J. Biol. Chem. *275*, 40517–40528. https://doi.org/10.1074/jbc.M006897200.

75. Tanaka, K., Kajiyama, N., Ishikura, K., Waga, S., Kikuchi, A., Ohtomo, K., Takagi, T., and Mizuno, S. (1999). Determination of the site of disulfide linkage between heavy and light chains of silk fibroin produced by Bombyx mori. Biochim. Biophys. Acta *1432*, 92–103. https://doi.org/10.1016/s0167-4838(99)00088-6.

76. Tanaka, K., Inoue, S., and Mizuno, S. (1999). Hydrophobic interaction of P25, containing Asn-linked oligosaccharide chains, with the H-L complex of silk fibroin produced by Bombyx mori. Insect Biochem. Mol. Biol. *29*, 269–276. https://doi.org/10.1016/s0965-1748(98)00135-0.

77. Hao, Z., Long, D., Zhang, Y., Umuhoza, D., Dai, J., Xu, Z., Zhang, G., Meng, W., Xiang, Z., and Zhao, A. (2021). New insight into the mechanism of in vivo fibroin self-assembly and secretion in the silkworm, Bombyx mori. Int. J. Biol. Macromol. *169*, 473–479. https://doi.org/10.1016/j.ijbiomac.2020.12.132.

78. Porter, D., Vollrath, F., and Shao, Z. (2005). Predicting the mechanical properties of spider silk as a model nanostructured polymer. Eur. Phys. J. E Soft Matter *16*, 199–206. https://doi.org/10.1140/epje/e2005-00021-2.

79. Liu, Q., Wang, F., Gu, Z., Ma, Q., and Hu, X. (2018). Exploring the Structural Transformation Mechanism of Chinese and Thailand Silk Fibroin Fibers and Formic-Acid Fabricated Silk Films. Int. J. Mol. Sci. *19*, 3309. https://doi.org/10.3390/ijms19113309.

80. Mortimer, B., Holland, C., and Vollrath, F. (2013). Forced Reeling of Bombyx mori Silk: Separating Behavior and Processing Conditions. Biomacromolecules *14*, 3653–3659. https://doi.org/10.1021/bm401013k.

81. Khan, M.M.R., Morikawa, H., Gotoh, Y., Miura, M., Ming, Z., Sato, Y., and Iwasa, M. (2008). Structural characteristics and properties of Bombyx mori silk fiber obtained by different artificial forcibly silking speeds. Int. J. Biol. Macromol. *42*, 264–270. https://doi.org/10.1016/j.ijbiomac.2007.12.001.

82. Omenetto, F.G., and Kaplan, D.L. (2010). New opportunities for an ancient material. Science *329*, 528–531. https://doi.org/10.1126/science.1188936.

83. Madsen, B., Shao, Z.Z., and Vollrath, F. (1999). Variability in the mechanical properties of spider silks on three levels: interspecific, intraspecific and intraindividual. Int. J. Biol. Macromol. *24*, 301–306. https://doi.org/10.1016/S0141-8130(98)00094-4.

84. Mortimer, B., Guan, J., Holland, C., Porter, D., and Vollrath, F. (2015). Linking naturally and unnaturally spun silks through the forced reeling of Bombyx mori. Acta Biomater. *11*, 247–255. https://doi.org/10.1016/j.actbio.2014.09.021.

85. Wang, Q., McArdle, P., Wang, S.L., Wilmington, R.L., Xing, Z., Greenwood, A., Cotten, M.L., Qazilbash, M.M., and Schniepp, H.C. (2022). Protein secondary structure in spider silk nanofibrils. Nat. Commun. *13*, 4329. https://doi.org/10.1038/s41467-022-31883-3.

86. Agnarsson, I., Kuntner, M., and Blackledge, T.A. (2010). Bioprospecting finds the toughest biological material: extraordinary silk from a giant riverine orb spider. PLoS One *5*, e11234. https://doi.org/10.1371/journal.pone.0011234.

87. Takakura, A., Beppu, K., Nishihara, T., Fukui, A., Kozeki, T., Namazu, T., Miyauchi, Y., and Itami, K. (2019). Strength of carbon nanotubes depends on their chemical structures. Nat. Commun. *10*, 3040. https://doi.org/10.1038/s41467-019-10959-7.

Matter, Volume *6*

Supplemental information

High-strength and ultra-tough whole spider silk fibers spun from transgenic silkworms

Junpeng Mi, Yizhong Zhou, Sanyuan Ma, Xingping Zhou, Shouying Xu, Yuchen Yang, Yuan Sun, Qingyou Xia, Hongnian Zhu, Suyang Wang, Luyang Tian, and Qing Meng

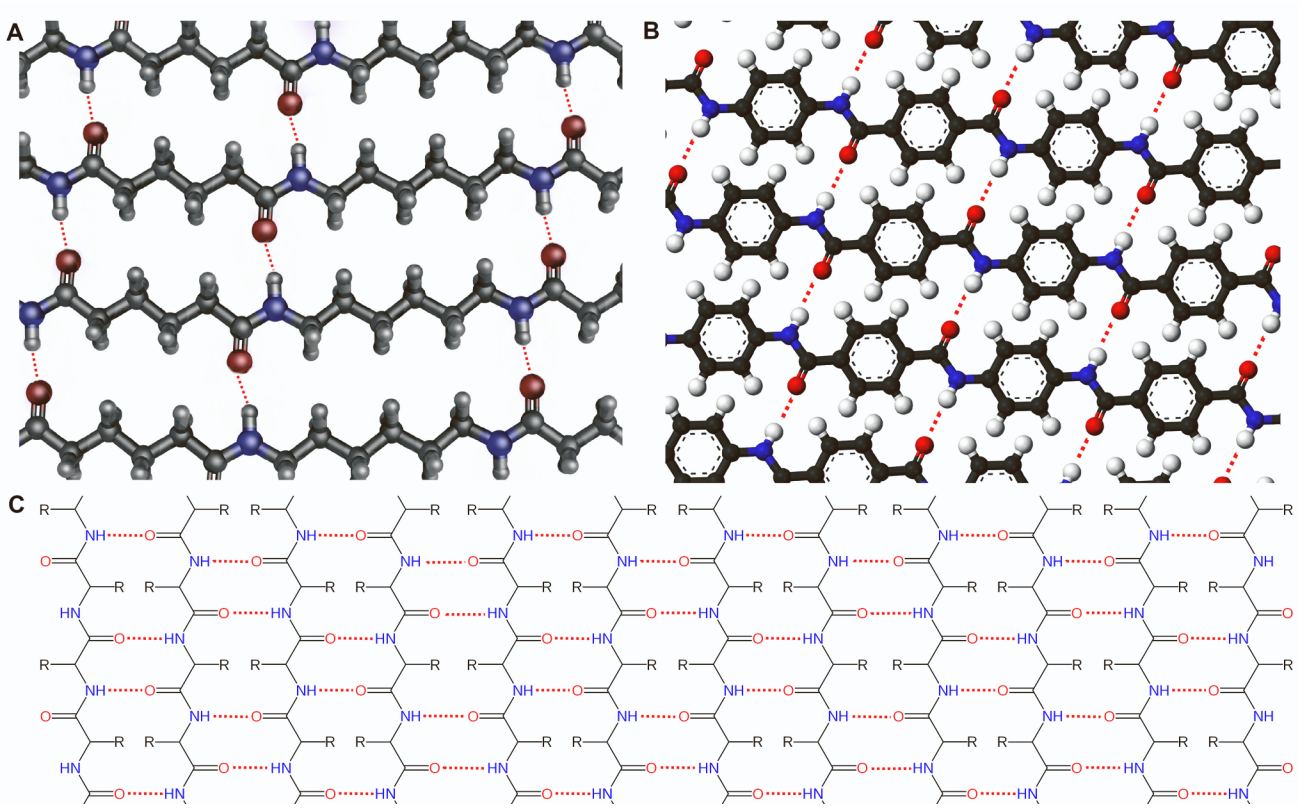

Figure S1. Molecular structure and distribution of hydrogen bonding in β-sheets of nylon, Kevlar, and spider silk.

(A) Molecular structure of nylon 66. The red dashed lines represent hydrogen bonds. The red color represents oxygen atoms and the blue color represents nitrogen atoms.

(B) Molecular structure of Kevlar. The red dashed lines represent hydrogen bonds. The ortho-hexagonal shape represents the benzene ring. The red color represents oxygen atoms and the blue color represents nitrogen atoms.

(C) Molecular structure of spider silk β-sheet. The red dashed lines represent hydrogen bonds. R represents the side chains of different amino acid residues.

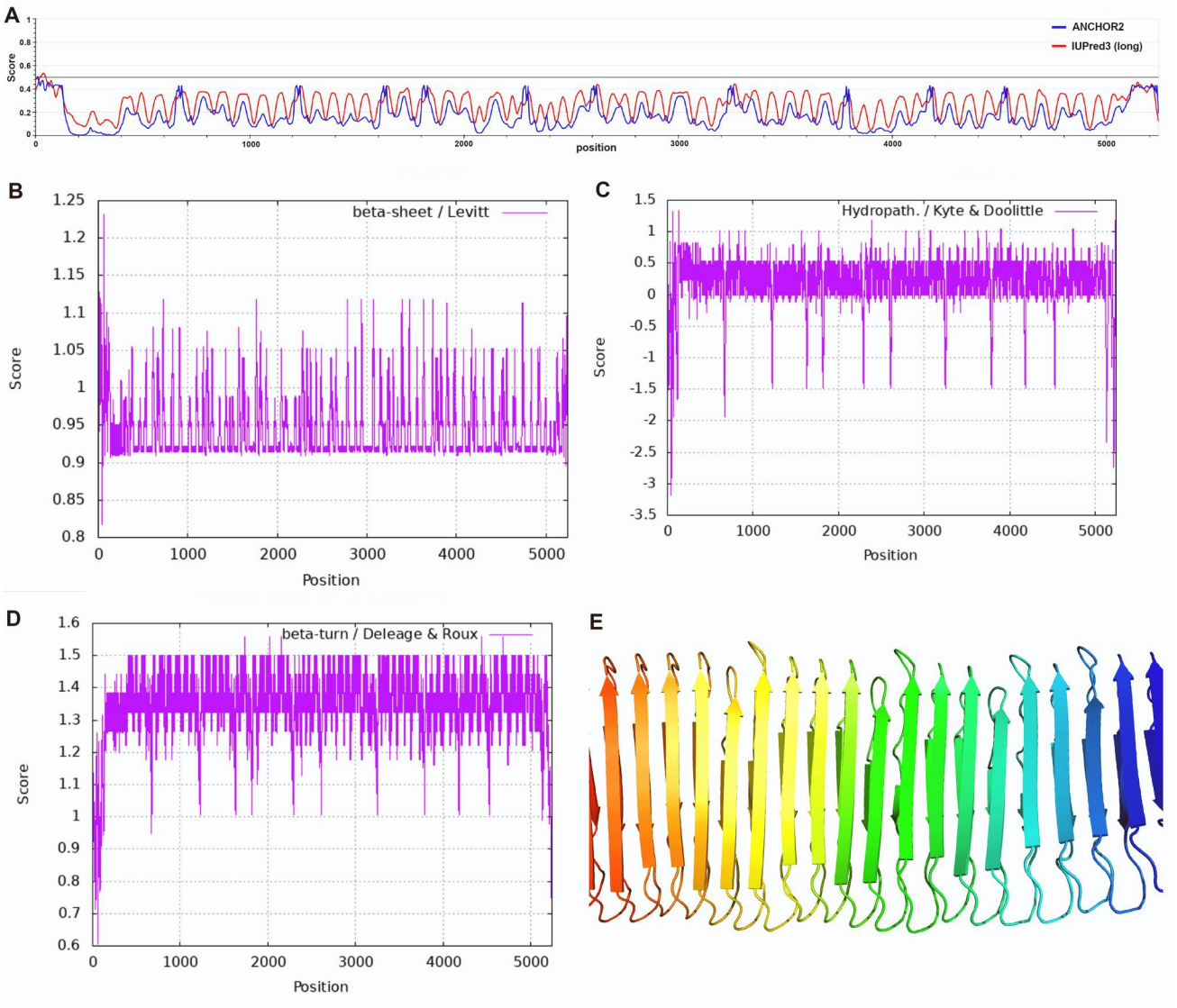

Figure S2. Molecular characterization of Fib-H.

(A) Analysis of the molecular characteristics of the disordered protein regions and the regions associated with protein disorder in Fib-H.

(B) Analysis of the distribution of β-sheet structures in Fib-H.

(C) Analysis of the distribution of hydrophilic amino acids in Fib-H.

(D) Analysis of the distribution of β-turns in Fib-H.

(E) Structural analysis of the repetitive region of Fib-H in the Bird-cherry ermine moth.

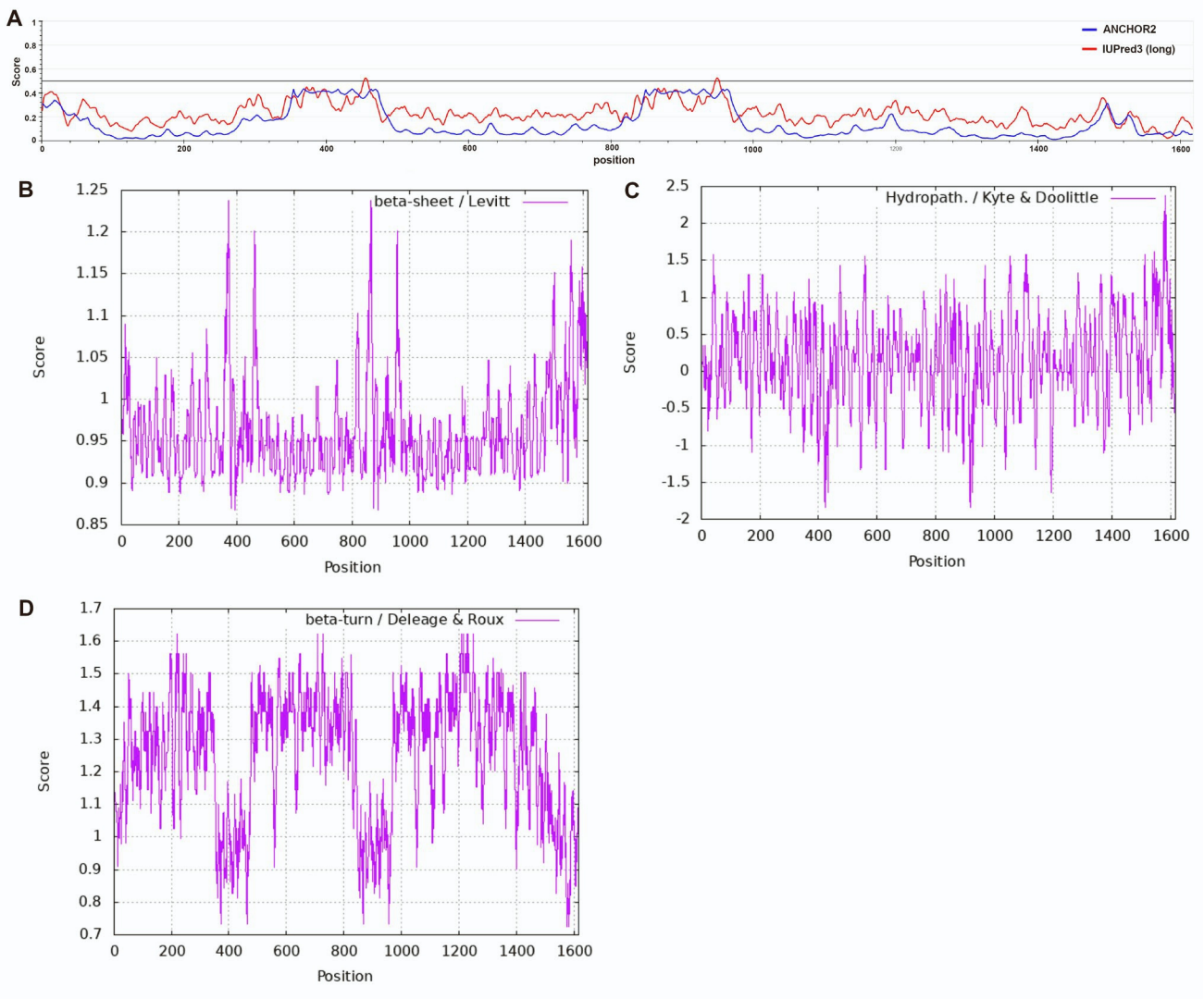

Figure S3. Molecular characterization of minor ampullate spidroin (MiSp).

(A) Analysis of the molecular characteristics of the disordered protein regions and the regions associated with protein disorder in MiSp.

(B) Analysis of the distribution of β-sheet structures in MiSp.

(C) Analysis of the distribution of hydrophilic amino acids in MiSp.

(D) Analysis of the distribution of β-turns in MiSp.

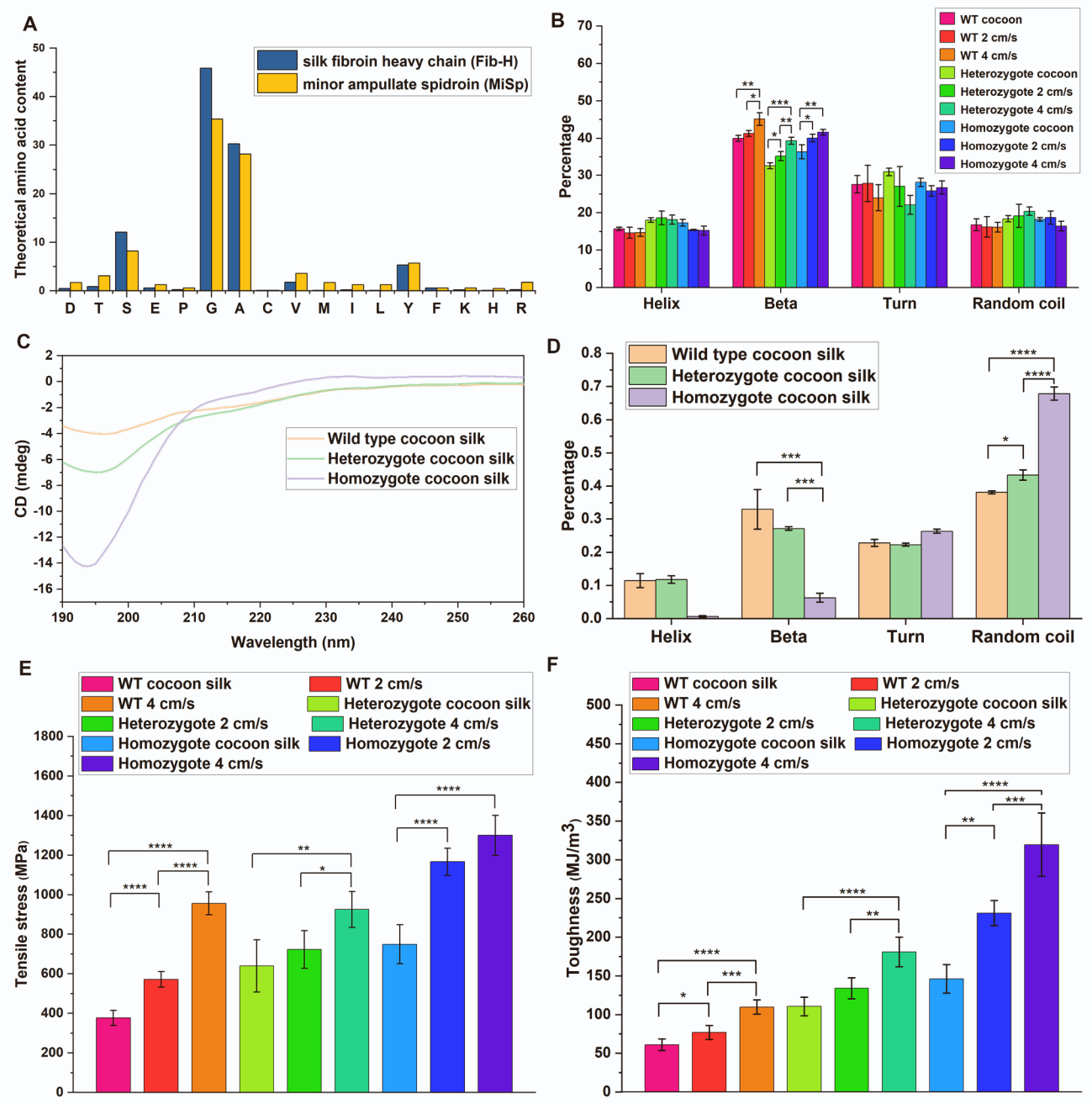

Figure S4. Analysis of the secondary structure and mechanical properties of silk fibers.

(A) Theoretical percentages of amino acid content for Fib-H and MiSp.

(B) Analysis of the secondary structure of fibers. Error bars represent standard deviations (n = 3).

(C) Circular dichroism (CD) spectra of the three silk protein solutions.

(D) Analysis of the secondary structure of the silk protein solutions. Error bars represent standard deviations (n = 3).

(E) Analysis of the tensile strength of silk fibers. Error bars represent standard deviations (n = 5).

(F) Analysis of the toughness of silk fibers. Error bars represent standard deviations (n = 5).

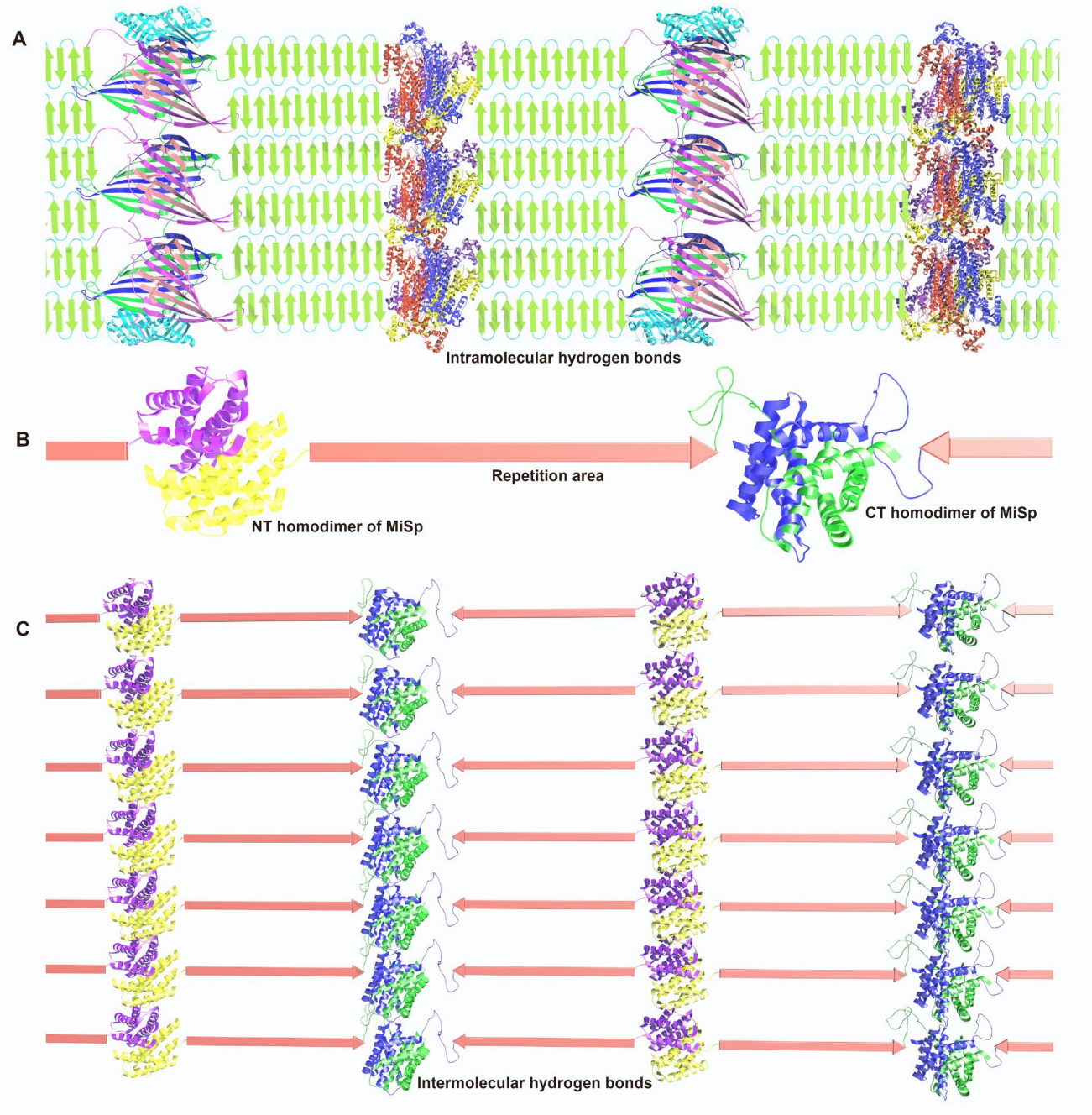

Figure S5. Illustration of molecular arrangements in silkworm silk and spider silk.

(A) Schematic diagram depicting the molecular arrangement between silk molecules in silkworm silk.

(B) Schematic diagram of the molecular head-to-tail linkage of MiSp.

(C) Schematic diagram depicting the molecular arrangement between silk molecules in MiSp silk fiber.

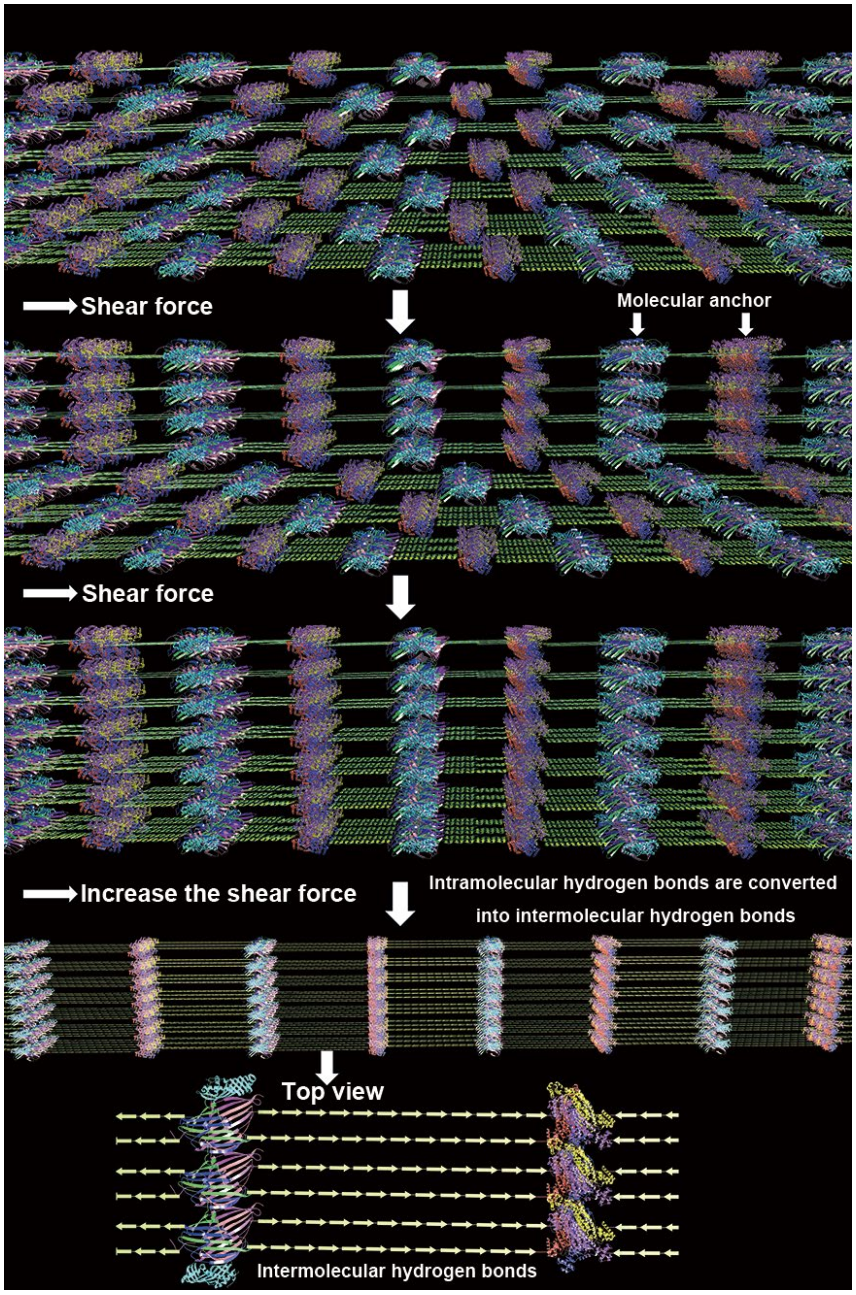

Figure S6. Schematic diagram of the shear force acting on silkworm silk.

The N-terminal homotetramer of Fib-H and the Fib-L homotetramer can act as “molecular anchors” to prevent excessive shear from rearranging molecules that are already neatly aligned. Excessive shear can induce the conversion of intramolecular hydrogen bonds to intermolecular hydrogen bonds in the repetitive region of Fib-H, thus increasing the cohesive energy density and ASMCED of the silk. The molecules in the silk shell are aligned, and the “molecular anchor” is fixed so that the molecules are not sliding relative to each other. Then, the sliding friction between molecules is transformed into static friction, which can effectively transfer the shear force to the next layer of molecules. Therefore, the shear effect decreases from the shell of the silk to the core of the silk axis.

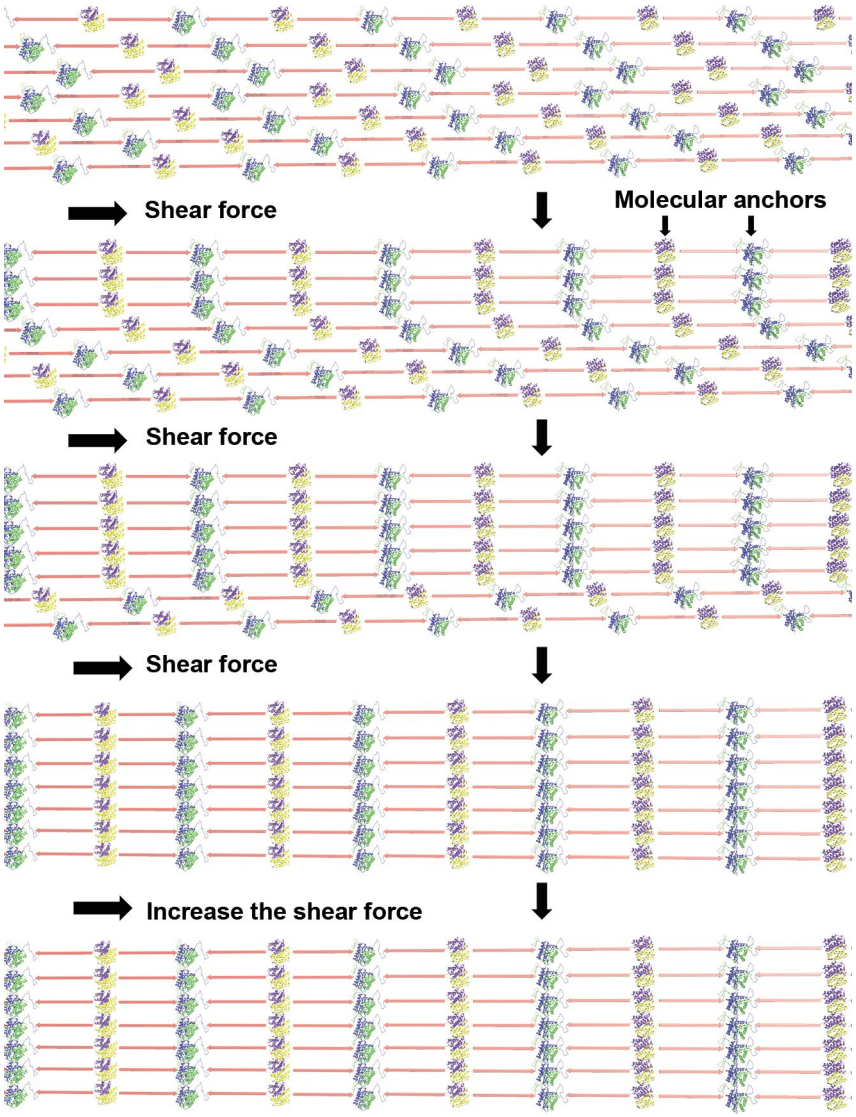

Figure S7. Schematic diagram of the shear force acting on MiSp.

The N-terminal and C-terminal homodimers of MiSp can act as “molecular anchors” to promote the alignment of protein molecules in response to shear forces. They also prevent excessive shear from realigning aligned molecules.

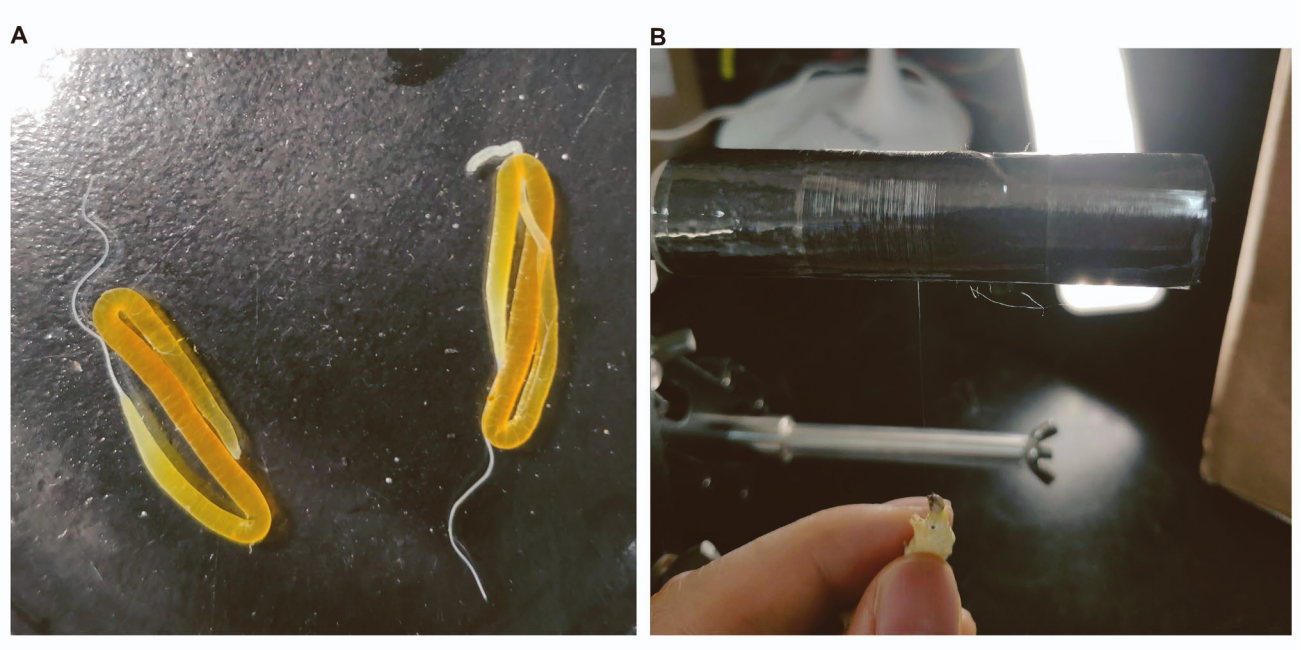

Figure S8. Photographs of silkworm silk glands and forced reeled silk.

(A) Silk glands observed during the cocooning process in silkworms.

(B) Image of forced reeled silk**.**

Table S1. Group Interaction Modeling (GIM) modelling parameters for silkworm silk and spider silk.

Silk type	Cohesive energy (kJ /mol) [1,2]	Van der Waal's volume (cc/mol) [1,2]	Cohesive energy density (kJ/cc)	INCBED (kJ/cc)	ASM-INCBED (kJ/cc)
Silkworm silk	49.2 [1]	34.93 [1]	1.41	0.21	1.2×10^{-23}
MiSp silk	50.2	38.73	1.30	1.07	6.9×10^{-23}

The cohesive energy and volume parameters for silkworm silk and spider silk were obtained from the published work[1,2]. Cohesive energy density was calculated based on these parameters. The intermolecular cohesive energy density, which arises from non-covalent bonds between silk molecules, was determined using the minimum structural model of silk. The MiSp repetitive region forming the intermolecular β-sheet accounts for 82.5% of the entire molecule. The accompanying table presents the volume occupied by 1 mole of silk and spider silk protein molecules, facilitating the calculation of the molecule count within a 1 cc volume. Dividing the intermolecular cohesive energy density (kJ/cc) by the molecule count within 1 cc yields the ASM-INCBED value. For a 1 cc volume, the number of silk molecules is approximately 1/34.93 mol, equivalent to 1/34.93 × 6.02 × 10^23 molecules, whereas the number of spider silk molecules is approximately 1/38.73 mol, equivalent to 1/38.73 × 6.02 × 10^23 molecules. Dividing the INCBED by the molecule count within 1 cc volume yields the ASM-INCBED value. Please note that intermolecular cohesive energy density primarily comprises non-covalent bonds between molecules. Hence, we equate intermolecular cohesive energy density with intermolecular non-covalent bond energy density (INCBED).

Table S2. Mechanical properties of silk fibers (reeling speeds of 2 and 4 cm/s).

Silk type	Diameter (μm)	Modulus (GPa)	Stress at break (MPa)	Strain at break (mm/mm)	Toughness (MJ/m^3)
WT cocoon silk	12.0 ± 0.8	10.3 ± 2.4	377.5 ± 38.1	0.22 ± 0.04	61.1 ± 7.5
WT 2 cm/s	10.5 ± 0.6	15.0 ± 2.6	572.0 ± 39.1	0.18 ± 0.03	76.9 ± 8.9
WT 4 cm/s	8.1 ± 0.3	28.3 ± 3.8	956.3 ± 57.9	0.15 ± 0.01	109.7 ± 9.1
Heterozygote cocoon silk	10.8 ± 0.9	16.1 ± 4.8	639.8 ± 132.5	0.24 ± 0.04	110.6 ± 12.0
Heterozygote 2 cm/s	8.7 ± 0.6	16.3 ± 3.7	722.8 ± 95.2	0.26 ± 0.03	134.0 ± 13.7
Heterozygote 4 cm/s	8.2 ± 0.8	21.2 ± 3.2	925.2 ± 90.8	0.27 ± 0.02	180.9 ± 19.1
Homozygote cocoon silk	12.6 ± 1.2	16.6 ± 3.8	749.1 ± 98.9	0.26 ± 0.05	146.1 ± 18.5
Homozygote 2 cm/s	12.8 ± 0.7	26.7 ± 3.	1166.8 ± 68.7	0.26 ± 0.03	231.1 ± 16.2
Homozygote 4 cm/s	12.4 ± 0.7	26.1 ± 0.9	1299.9 ± 101.6	0.33 ± 0.04	319.5 ± 41.0
Nylon 66 [3,4]			750 - 950	0.18	80
Kevlar 49 [3,4]			3600	0.027	50
***Caerostris darwini* silk**[5]			1652 ± 208	0.52 ± 0.22	354 ± 93
Aciniform Silk[6]	0.35 ± 0.1		678 ± 56	0.86 ± 0.03	376 ± 39

Data are means and standard deviations (n = 5).

Table S3. Percentage of silks secondary structure.

Silk type	Helix	Beta	Turn	Random coil
WT cocoon silk	15.7 ± 0.4	39.9 ± 0.8	27.6 ± 2.3	16.8 ± 1.6
WT 2 cm/s	14.6 ± 1.5	41.3 ± 0.8	27.9 ± 4.9	16.2 ±2.7
WT 4 cm/s	14.8 ± 1.0	45.1 ±1.7	24.0 ± 3.5	16.2 ± 1.3
Heterozygote cocoon silk	18.0 ± 0.6	32.6 ± 0.8	30.9 ± 1.1	18.4 ± 0.8
Heterozygote 2 cm/s	18.6 ± 1.8	35.2 ± 1.2	27.0 ± 5.4	19.1 ± 3.1
Heterozygote 4 cm/s	18.1 ± 1.2	39.3 ± 0.9	22.1 ± 2.5	20.4 ± 1.1
Homozygote cocoon silk	17.3 ± 0.9	36.3 ± 01.9	28.1 ± 1.1	18.2 ± 0.5
Homozygote 2 cm/s	15.4 ± 0.1	40.0 ± 1.0	25.8 ± 1.4	18.7 ± 1.7
Homozygote 4 cm/s	15.2 ± 1.2	41.6 ± 0.8	26.7 ± 1.8	16.4 ± 1.3

Data are means and standard deviations (n = 3).

Supplemental experimental procedures

All experimental methods can be found in the 'Experimental Procedures' section of the manuscript. There are no additional experiments or information in the supplemental documents that are separate from the main manuscript.

References

1. Guan, J., Wang, Y., Mortimer, B., Holland, C., Shao, Z., Porter, D., and Vollrath, F. (2016). Glass transitions in native silk fibres studied by dynamic mechanical thermal analysis. Soft Matter *12*, 5926-5936. 10.1039/c6sm00019c.
2. Porter, D., Vollrath, F., and Shao, Z. (2005). Predicting the mechanical properties of spider silk as a model nanostructured polymer. Eur Phys J E Soft Matter *16*, 199-206. 10.1140/epje/e2005-00021-2.
3. Heim, M., Keerl, D., and Scheibel, T. (2009). Spider silk: from soluble protein to extraordinary fiber. Angew Chem Int Ed Engl *48*, 3584-3596. 10.1002/anie.200803341.
4. Li, J., Li, S., Huang, J., Khan, A.Q., An, B., Zhou, X., Liu, Z., and Zhu, M. (2022). Spider Silk-Inspired Artificial Fibers. Adv Sci (Weinh) *9*, e2103965. 10.1002/advs.202103965.
5. Agnarsson, I., Kuntner, M., and Blackledge, T.A. (2010). Bioprospecting finds the toughest biological material: extraordinary silk from a giant riverine orb spider. PLoS One *5*, e11234. 10.1371/journal.pone.0011234.
6. Hayashi, C.Y., Blackledge, T.A., and Lewis, R.V. (2004). Molecular and mechanical characterization of aciniform silk: uniformity of iterated sequence modules in a novel member of the spider silk fibroin gene family. Mol Biol Evol *21*, 1950-1959. 10.1093/molbev/msh204.